



The role of sediment supply in large-scale stratigraphic architecture of ancient Gilbert-type deltas (Pliocene Siena-Radicofani Basin, Italy)

This is the peer reviewed version of the following article:

Original:

Martini, I., Ambrosetti, E., Sandrelli, F. (2017). The role of sediment supply in large-scale stratigraphic architecture of ancient Gilbert-type deltas (Pliocene Siena-Radicofani Basin, Italy). *SEDIMENTARY GEOLOGY*, 350, 23-41 [10.1016/j.sedgeo.2017.01.006].

Availability:

This version is available <http://hdl.handle.net/11365/1005844> since 2017-04-28T16:19:35Z

Published:

DOI:10.1016/j.sedgeo.2017.01.006

Terms of use:

Open Access

The terms and conditions for the reuse of this version of the manuscript are specified in the publishing policy. Works made available under a Creative Commons license can be used according to the terms and conditions of said license.

For all terms of use and more information see the publisher's website.

(Article begins on next page)

1 **The role of sediment supply in large-scale stratigraphic architecture of ancient**
2 **Gilbert-type deltas (Pliocene Siena-Radicofani Basin, Italy)**

3

4 Ivan Martini^{1*}, Elisa Ambrosetti¹, Fabio Sandrelli¹

5

6 ¹Dipartimento di Scienze Fisiche, della Terra e dell’Ambiente, Università di Siena, Via Laterina 8, 53100 Siena (Italy)

7 Corresponding Author: martini.ivan@unisi.it

8

9 **Abstract**

10 Aggradation, progradation and retrogradation are the main patterns that define the large-scale
11 architecture of Gilbert-type deltas. These patterns are governed by the ratio between the variation in
12 accommodation space and sediment supply experienced during delta growth. Sediment supply
13 variations are difficult to estimate in ancient settings; hence, it is rarely possible to assess its
14 significance in the large-scale stratigraphic architecture of Gilbert-type deltas. This paper presents a
15 stratigraphic analysis of a Pliocene deltaic complex composed of two coeval and narrowly spaced
16 deltaic branches. The two branches recorded the same tectonic- and climate-induced accommodation
17 space variations. As a result, this deltaic complex represents a natural laboratory for testing the effects
18 of sediment supply variations on the stratigraphic architecture of Gilbert-type deltas. The field data
19 suggest that a sediment supply which is able to counteract the accommodation generated over time
20 promotes the aggradational/progradational attitude of Gilbert-type deltas, as well as the development of
21 thick foreset deposits. By contrast, if the sediment supply is not sufficient for counterbalancing the
22 generated accommodation, an aggradational/retrogradational stratigraphic architecture is promoted. In
23 this case, the deltaic system is forced to withdraw during the different phases of generation of
24 accommodation, with the subsequent flooding of previously deposited sub-horizontal topset deposits
25 (i.e., the delta plain). The subsequent deltaic progradation occurs above these deposits and,

26 consequently, the available space for foresets growth is limited to the water depth between the base-
27 level and the older delta plain. This leads to the vertical stacking of relatively thin deltaic deposits with
28 an overall aggradational/retrogradational attitude.

29

30 *Keywords:* Gilbert-type delta, shoal-water delta, delta stratigraphic arrangement, sediment supply,
31 accommodation.

32

33 **1. Introduction**

34

35 Gilbert-type deltas have been extensively described in many tectonically active and quiescent basins
36 (e.g., Ethridge and Wescott, 1984; Colella, 1988; Nemec and Steel, 1988; Leren et al., 2010) and have
37 attracted the attention of sedimentary geologists predominantly for their importance as indicators of the
38 infill history of basins. This is particularly relevant for coarse-clastic basin margins, where bio-
39 stratigraphic age control is generally poor and the stratigraphic arrangement of Gilbert-type deltas has
40 been used as a tool for refining the reconstruction of basin fill patterns and basin subsidence kinematics
41 (Postma, 1995).

42 The large-scale architecture of Gilbert-type deltas is defined by three main patterns: progradation,
43 aggradation and retrogradation (e.g., Postma, 1995; Marzo and Steel, 2000). These patterns are
44 generally identified by the trajectory of the topset/foreset transition point (also called “topset
45 breakpoint path” by some authors, e.g., Backert et al., 2009) along the sedimentary succession
46 (Helland-Hansen and Martinsen, 1996; Mortimer et al., 2005). These stratigraphic patterns are
47 essentially governed by two allocyclic driving factors: i) the accommodation space variations, and ii)
48 the type and amount of sediments supplied to the deltaic systems by rivers (Posamentier and Allen,
49 1993; Dorsey et al., 1995; Postma, 1995; Bijkerk et al., 2014). Autocyclic processes (e.g., delta-lobe

50 switching) may secondarily influence the architecture of deltas, although they generally do not
51 dramatically modify the overprint given by allocyclic driving factors to the final stratigraphic
52 architecture.

53 The creation/degradation of accommodation space results from the combination of global sea-level
54 variations and vertical movements within the basin. In turn, the combination of global sea-level
55 variations, basin subsidence and sediment supply define the stratigraphic architecture of sedimentary
56 successions and the shoreline trajectory pattern (cf., Posamentier and Allen, 1999; Coe et al., 2002;
57 Catuneanu, 2002). Global sea-level variations are easily predictable from the Pliocene to present (Haq
58 et al., 1987; Miller et al., 2005) and the basin subsidence history can be deduced by
59 micropalaeontological, structural, seismic and geophysical data. On the contrary, the type and amount
60 of sediment supplied to deltas are difficult to estimate in ancient settings, even though they play a
61 crucial role in the formation and growth of deltas (López-Blanco et al., 2000; Marzo and Steel, 2000;
62 Carvajal et al., 2009; Bijkerk et al., 2014). Variations in sediment yield can be connected for several
63 factors, such as climatic changes, tectonics, geology of the drainage basin, inherited basin relief, etc.
64 (cf., Schumm and Lichty, 1965), which often act unpredictably.

65 The aim of this paper is to understand the role of sediment supply on the stratigraphic architecture of
66 ancient Gilbert-type deltas. For this purpose, a Pliocene Gilbert-delta complex located in the Siena-
67 Radicofani Basin (Tuscany, Italy) has been investigated in accordance with sedimentological and
68 stratigraphic criteria. The delta complex is composed of two different branches, situated ~300 m apart,
69 and supposed coeval based on the lateral tracing of two key stratigraphic surfaces that mark the
70 beginning and the end of the Gilbert-type related deposition. The two branches show an overall similar
71 stratigraphic evolution, with basal shoal-water delta deposits passing upward to Gilbert-type delta
72 deposits, which are in turn abruptly overlain by shoal-water delta deposits. However, the Gilbert-type
73 delta deposits in the two branches display a marked difference in their stratigraphic arrangement.

74 The coeval timing of the two delta branches ensures that climate-induced base-level fluctuations
75 influenced the delta complex built up in the same way. Moreover, the shoal-water delta deposits at the
76 base and top of the succession narrowly constrain the accommodation space experienced during
77 Gilbert-delta build-up, suggesting that subsidence acted uniformly in the area during deposition.
78 Consequently, it is considered that the observed differences in the stratigraphic architecture are only
79 attributable to differential sediment supply feeding the different delta branches.

80

81 **2. Geological setting**

82

83 The study area is located in the central part of the Siena-Radicofani Basin, close to the traditionally
84 accepted boundary between the Siena and Radicofani sub-basins (southern Tuscany, Italy; Fig. 1A, B).
85 These sub-basins have been considered as independent basins for a long time. Recently, however,
86 Brogi (2011) demonstrated that they belong to the same tectonic depression and for this reason the term
87 “sub-basins” is adopted. The Siena-Radicofani Basin (which also includes the Casino sub-basin to the
88 north) is one of the most important post-collisional basins of the inner Northern Apennines (Costantini
89 et al., 2009). Post-collisional basins correspond to a series of NNW-SSE trending tectonic depressions
90 developed since the middle Miocene (Jolivet et al., 1998; Brunet et al., 2000), in which continental and
91 marine sediments accumulated since the Miocene until the Quaternary.

92 The Siena-Radicofani Basin is traditionally interpreted as having developed in extensional settings and
93 records a basin-and-range structural architecture (Martini and Sagri, 1993; Carmignani et al., 1995;
94 Jolivet et al., 1998; Pascucci et al., 1999; Carmignani et al., 2001). Brogi (2011) proposed a more
95 complex history, which sees the basin originating due to the activity of Serravallian/late Messinian
96 staircase extensional detachments. These produced a bowl-shaped structural depression, which is
97 partially modified by high-angle normal fault systems active during the Pliocene. Other authors

98 interpreted the Basin as a thrust-top basin developed in a compressional tectonic setting (Finetti et al.,
99 2001; Bonini and Sani, 2002).

100

101 *2.1 Neogene sedimentation*

102 Sedimentation in the Siena-Radicofani Basin starts in the late Miocene when deposition of a fluvio-
103 lacustrine succession occurred. Miocene deposits unconformably overlie pre-Neogene bedrock and are
104 presently exposed in limited areas. These sediments are in turn overlain unconformably by Pliocene
105 deposits (Costantini et al., 2009) which accumulated since the early Zanclean until the late
106 Piacenzian/earliest Gelasian (Bossio et al., 1992; Martini et al., 2011, 2013, 2016; Arragoni et al.,
107 2012; Martini and Sandrelli, 2015).

108 The Pliocene succession is mainly represented by nearshore marine deposits close to basin margins,
109 which pass basinwards to offshore fines. Episodes of continental sedimentation have been reported in
110 the lower part of the Pliocene succession close to the Siena sub-basin margins (Bossio et al., 1992,
111 1993; Aldinucci et al., 2007; Manganelli et al., 2010, 2011; Martini et al., 2011; Bianchi et al., 2013).
112 Individual sub-basins recorded different infilling histories, generally related to the time intervals when
113 deposition occurred. Synthetic stratigraphic columns of the sedimentary successions exposed in the
114 central sectors of the Siena and Radicofani sub-basin are proposed in Fig. 1C. Figure 1C also reports
115 the stratigraphic column of the sedimentary succession exposed in correspondence to the bedrock high
116 that marks the traditionally accepted Siena/Radicofani sub-basins boundary (i.e, the so called “Pienza
117 high”, data derived from Marini, 2001; Antoni et al., 2005). Among the several and marked differences
118 in the depositional infilling history of these areas, it is important to highlight that marine settings
119 persisted in basinal areas during the Pliocene. A low-magnitude intra-Pliocene base-level fall (occurred
120 within the MPI3 biozone) is recorded only in the surrounding of the “Pienza high”, where lacustrine
121 limestones and fluvial conglomerate occur within the Pliocene succession. Continental settings in

122 which these deposits accumulated have been interrupted by a relative sea-level rise occurred at top of
123 the Zanclean (MPI4 biozone) that restored marine settings (Marini, 2001).
124 Marine settings ended due to a regional uplift which affected southern Tuscany since the Piacenzian
125 (Marinelli, 1975; Bossio et al., 1993). Quaternary deposition is documented by discontinuous outcrops
126 of sandy-gravelly alluvial deposits (Aldinucci et al., 2007; Bianchi et al., 2013; Brogi et al., 2014).
127 The investigated area is located close to the “Pienza high” and previous stratigraphic studies have been
128 performed in this area adopting lithostratigraphic criteria (Bonini and Sani, 2002; Antoni et al., 2005).
129 The succession deposited during the Zanclean (MNN14/15 biozone of nannoplankton biostratigraphy;
130 Martini et al., 2015) and according to Bonini and Sani (2002) and Antoni et al. (2005) it is mainly
131 composed of coarse-grained and steeply inclined (up to 30°) conglomerate beds overlain by sub-
132 horizontal sandstone. Bonini and Sani (2002) interpreted the angular unconformity between the
133 conglomerate and the sandstone as connected to an intra-Pliocene uplifting pulse.

134

135 **3. Methods**

136

137 The study uses conventional geological field methods, including: i) mapping based on facies
138 association concepts (at 1:5000 scale); ii) bed-by-bed sedimentological logging of twelve sections
139 (about 320 m of measured succession); iii) collection of palaeocurrent indicators; and iv) line-drawing
140 of architectures on photomosaics of four selected outcrops (up to 400 m long and 80 m high). The
141 location of measured sections, as well as of the outcrops selected for line-drawings, is reported on
142 Figure 2. The area is vegetated by tall trees, thus offering limited opportunities to take good
143 photographic records of extensive outcrops. In order to overcome this problem, large outcrops are
144 featured as line-drawings and important features are detailed in close-up photos.

145 The sedimentological analysis is based on the concept of facies association, i.e., assemblages of
146 spatially and genetically related facies that are the expression of different sedimentary environments
147 (Walker and James, 1992). The descriptive sedimentological terminology is from Harms et al. (1975,
148 1982) and Collinson et al. (2006).

149 The term “flooding surface” is used in accordance with its classical meaning (cf., Van Wagoner et al.,
150 1988), i.e., the surface connected to a transgressive pulse that separates shallower-water strata below
151 from deeper-water strata above. However, in deltaic settings, autocyclic factors (i.e., not connected
152 with base-level fluctuations) can produce vertical facies superimposition that resembles those typically
153 connected to flooding surfaces. The term “deactivation surfaces” has been introduced to describe
154 settings where vertical facies superimpositions have an ambiguous significance and could be related
155 either to flooding events or to autocyclic lobe avulsion processes.

156 The term EDU (elementary deltaic unit) is used according to Ambrosetti et al. (2017), i.e., to indicate
157 an assemblage of vertically stacked and genetically related facies that document the progradation of the
158 deltaic system. EDUs are the stratigraphic expression of delta lobes, i.e., the sedimentary body forming
159 at the river mouth. Individual EDUs are bounded by flooding/deactivation surfaces and, consequently,
160 EDUs are equivalent to parasequences only if the progradation is interrupted by flooding surfaces,
161 whereas they do not coincide with parasequences if the progradational trend is interrupted by
162 deactivation surfaces connected to autocyclic processes, such as delta lobe switching. The term
163 “parasequence” is used in accordance with the definition of Van Wagoner et al. (1988) taking into
164 account the suggestions of Arnott (1995).

165 The term “delta branch” is used to indicate the area interested by deltaic deposition in which the
166 sediments have been provided by the same distributive system. As a consequence, each delta branch
167 record a complex depositional history, that includes lobe superimposition, lateral lobes stacking and
168 lobe shifts.

169

170 **4. Results**

171

172 Ten facies associations have been identified on the basis of sedimentological and stratigraphic features.
173 Each facies association is representative of a well-defined depositional environment; their features are
174 described and interpreted below and summarised in Table 1. Facies associations are described in the
175 main text from distal to proximal. Eight facies associations are the expression of deposition in a deltaic
176 environment, one is the expression of wave- winnowing processes acted in nearshore settings, and
177 another one is the expression of continental deposition.

178 The distribution of sedimentary facies (Fig. 2) document that Gilbert-type deposition occurred in two
179 deltaic branches (hereafter DB1 and DB2). As commonly observed in deltaic systems, coarse-grained
180 facies typify the axial portion of each delta branch (see Fig. 2), while finer sediments occur in distal
181 (pro-delta) and lateral (interlobe) positions. The two delta branches are spaced at about 300 m in
182 basinward positions, while they are in contact with each other in landward position. Consequently, the
183 spatial distribution of the two branches resembles two divergent aprons with the apical position located
184 in the same area.

185 Gilbert-type deposits are sandwiched between shoal-water deltaic deposits in both delta branches. The
186 stratigraphic boundaries of the Gilbert-type deposits correspond to two surfaces that can be traced
187 laterally throughout the entire investigated area and for this reason it has been used as a key surface for
188 lateral correlation between the two delta branches. They are named TS1 (lower boundary) and TS2
189 (upper boundary). Surface TS1 is associated with: i) wave-winnowed lag deposits flooring a low-relief
190 erosional surface; and ii) the drowning of the basal shoal-water deltaic system. As a consequence, TS1
191 corresponds to a transgressive surface associated with a major flooding event. Surface TS2 is also
192 connected with wave-winnowed lag deposits flooring an erosional surface and documenting a

193 transgressive event, but it also marks the abrupt deposition of shallower deposits (shoal-water delta
194 sediments) on top of bottomset and foreset deposits (see Fig. 8A,B). As a consequence, TS2 can be
195 interpreted as a composite surface originated due to a relative sea-level fall (responsible for the
196 superimposition of shallower facies above deeper one) combined with a subsequent transgression.
197 These two events are also recognized in the surrounding area (see Fig. 1C, “Pienza High” stratigraphy),
198 where they have led to the localized deposition of continental lacustrine sediments above marine
199 deposits, which are in turn overlain by shoreface sandstones. The detailed stratigraphic architecture of
200 each delta branch is described in section 4.2.

201

202 **4.1 Sedimentology**

203 **4.1.1 Offshore to prodelta deposits**

204 *Description*

205 These deposits consist of thick and monotonous successions of grey mudstone, rarely containing cm-
206 thick and tabular silty-sandstone beds. Mudstone beds are tabular and generally structureless due to the
207 pervasive bioturbation, while only occasionally a faint of lamination is observable. Mudstone beds are
208 generally poor in organic matter and locally contain marine mollusks (e.g., *Chlamys*, *Venus*,
209 *Naticarius*, etc.). The sandstone beds show sharp bases and tops and they are normally graded and
210 internally structureless or plane-parallel laminated. Low-angle cross-laminations can also be observed
211 at time in the upper part of the beds. Organic debris (e.g., plant, wood and leaves) and clay chips occur
212 occasionally in the basal part of the beds.

213

214 *Interpretation*

215 These deposits are interpreted as the expression of deposition in an open marine setting that is
216 relatively close to a shoreline and/or to fluvial inputs. The predominance of fine-grained sediments

217 suggests a deposition due to suspension fallout in offshore/prodelta marine setting (Johnson and
218 Baldwin, 1996). The uncommon sandstone beds were probably emplaced by major hyperpycnal flows
219 generated by river floods, where the genetic connection with river mouths is supported by the
220 occurrence of plants remains, as commonly documented in similar settings (e.g., Plink-Björklund and
221 Steel, 2004; Martini and Sandrelli, 2015).

222

223 **4.1.2 Delta front deposits of shoal-type deltas**

224 *Description*

225 This facies association predominantly consists of poorly- to moderately-sorted sandstone with
226 subordinated siltstone and conglomerate, forming coarsening-upward units up to 5-10 m thick,
227 characterized by tabular to slightly convex upward geometries at outcrop scale (Fig. 3A). Sandstone are
228 mainly expressed by two facies: i) thick (0.5-2 m) plane-parallel laminated beds, locally structureless
229 due to intense bioturbation, often forming m-thick amalgamated sandy packages; ii) low-angle cross-
230 laminated sandstone and gravelly sandstone. The former facies typical typify the lower part of
231 coarsening-upward units, while the latter the upper one. Shell-rich sandstone beds, with bivalve in life
232 position (including *Pinnidae*, Fig. 3B) often occur. Siltstone beds (cm-thick) typically occur in the
233 lower portion of coarsening-upward units and they are rich in sandy matrix, plane-parallel laminated
234 and poorly bioturbated. Plant debris and leaves remains are common both in the sandstone and the
235 siltstone beds.

236

237 *Interpretation*

238 The features of this facies association indicates that deposition occurred in a proximal delta front
239 environment of shoal-water type deltas, where depositional processes are dominated by frequent and
240 conspicuous sediment supply from a land-derived source (i.e., fluvial input). This limits the deposition

241 of fines, that are then pushed out in more distal settings. The deltaic nature of these deposits is also
242 supported by: i) the moderate sorting of sediments; ii) the common occurrence of terrestrial plant
243 remains, indicating a close terrestrial source of sediment; and iii) the overall geometries, typical of
244 delta lobes of shoal-water deltas.

245 The thick plane-parallel laminated sandstone packages are also typical of such environments and they
246 result from sustained underflows emanated from river mouths during river floods (Plink-Björklund and
247 Steel, 2004; Petter and Steel, 2006; Martini and Sandrelli, 2015). The features of siltstone beds (i.e.,
248 preservation of laminae and scarce bioturbation) suggest higher sedimentation rates (Martini and
249 Sandrelli, 2015), compatible with an emplacement related to land-derived low-density hypo- and
250 hyper-pycnal flows during stages of low discharge (Nemec, 1995). Shell-rich beds are representative of
251 stages of low sediment supply, when infaunal organisms can colonize the sea-floor. These stages are
252 attributed to transgressive pulses or to the temporary deactivation of the deltaic system.

253

254 **4.1.3 Mouth-bar deposits of shoal-type deltas**

255 *Description*

256 Deposits of this facies association typically overlies delta front deposits and consist of sandstone, with
257 subordinated conglomerate and gravelly sandstone (Fig. 3C). Fines are generally uncommon. Mouth-
258 bar deposits are arranged in 2-5 m thick units, characterized by coarsening-upward trends and well-
259 marked convex upward geometries at outcrop scale.

260 Mouth-bar deposits mainly consist of: i) plane-parallel stratified sandstone beds, often showing a basal
261 erosional scour, marked by the alignment of granules and pebbles; ii) dm-thick, normally graded,
262 structureless to plane-parallel and/or planar cross-stratified gravelly and coarse-grained sandstones,
263 with occasional mud clasts; iii) fine-grained and (symmetrical) rippled sandstones, that usually occur in
264 the upper part of the mouth-bar successions; iv) single-clasts alignments of gravels (pebble- to cobble-

265 sized), overlying slight erosional scours and overlaid in turn by finer-grained sediments (medium- to
266 fine-grained sandstone); and v) cm-thick massive to plane-parallel laminated sandy mudstone beds.

267

268 *Interpretation*

269 The overall features of this facies association (including the geometries, the stratigraphic position in
270 respect to delta front deposits, the coarsening-upward trend and the constituent facies) suggest that
271 sedimentation occurred in a mouth-bar environment, where sediments are directly supplied by
272 distributary channels. In these settings, the deposition is mainly related to sustained underflows
273 connected to river-related floods (i.e., hyperpycnal flows; Mulder and Alexander, 2001; Mulder et al.,
274 2003; Plink-Björklund and Steel, 2004; Petter and Steel, 2006; Olariu et al., 2010). Mouth-bar deposits
275 were at times reworked by fair-weather waves, as revealed by rippled sandstone, confirming that the
276 deposition occurred in relative shallow settings (above fair-weather wave base). Single-clast alignments
277 of gravels are the expression of residual lags connected to wave-winnowing processes during
278 transgressive pulses.

279

280 **4.1.4 Distributary channel deposits of shoal-type deltas**

281 *Description*

282 These deposits consist mainly of sandy conglomerate with subordinate sandstones arranged in fining-
283 upward lithosomes, forming erosional based and lens-shaped bodies, up to 2-3 m thick and 3-10 m
284 wide (Fig. 3C). Distributary channel deposits erosionally overlay mouth-bar deposits and show concave
285 upward bases and flat tops (Fig. 3C). At places, internal erosional surfaces are recognized within
286 distributary channel deposits.

287 Gravels are pebble- to cobble-sized and form 20-30 cm thick clast-supported beds, structureless to
288 crudely plane-parallel stratified. Clast imbrications (b(i)a(t) and a(i)a(p)) sometimes occur. Gravel beds

289 occasionally grade into massive or plane-parallel laminated coarse-grained sandstones. Individual beds
290 are typically amalgamated and clasts are often encrusted by barnacles showing no evidence of
291 reworking.

292

293 *Interpretation*

294 Based on the geometrical features, the fining-upward trend and the stratigraphic position, these deposits
295 are interpreted as distributary channel-fill deposits (Li and Bhattacharya, 2014). Distributary channels
296 represent the prolongation of river channels within the delta plain and supply sediments directly to the
297 mouth-bars and to the deltaic system.

298 Sedimentary facies resemble the typical facies recognizable in fluvial channel-fill deposits (Smith,
299 1974; Bridge, 2003), except for the clasts encrusted by barnacles that document the close genetic
300 relationship between the distributary channel deposits and the marine deltaic environment. The fining-
301 upward trend is indicative of the progressive infilling and abandonment of channels and internal
302 erosional surfaces suggest a multi-storey infill history (Ambrosetti et al., 2017).

303

304 **4.1.5 Bottomset deposits of Gilbert-type deltas**

305 *Description*

306 These deposits consist of poorly sorted sandstone with subordinate silty mudstone beds, typically sub-
307 horizontal to gently inclined seaward (0 to 5°, Fig. 4A). Bottomset deposits commonly occur directly
308 downdip and stratigraphically below toset and foreset deposits (Fig. 4A).

309 Sandstone are fine-grained, weakly sorted, structureless or faintly plane-parallel laminated (Fig. 4B, C).

310 Sandstone beds commonly contain isolated and rounded gravel clasts, dispersed within beds or
311 segregated into flat stringers (Fig. 4B, C). Mudstone beds are thin and discontinuous, often massive due
312 to bioturbation.

313

314 *Interpretation*

315 Features of this facies association and the genetic relation with toeset and foreset deposits suggest the
316 deposition in delta bottomset settings of Gilbert-type delta lobes (Colella, 1988; Massari and Colella,
317 1988; Sohn et al., 1997). Depositional processes in this environment are strongly influenced by the
318 decrease in delta slope occurring at the transition between Gilbert-delta foreset and bottomset, causing
319 the deposition by the dumping of sand load from high-density turbidity currents (*sensu* Lowe, 1982).
320 Isolated gravels within sandstone beds could be debris-fall “outrunners” (Nemec, 1990; Sohn et al.,
321 1997) or clasts rolled in isolation by the sandy turbidity currents (Postma and Roep, 1985). Mudstone
322 beds were emplaced due to low-density hypo- and hyper-pycnal flows connected to river-mouths.

323

324 **4.1.6 Toeset deposits of Gilbert-type deltas**

325 *Description*

326 These deposits consist of conglomerate with subordinate sandstone, typically sub-horizontal to gently
327 inclined seaward (0 to 10°). Toeset deposits occur above bottomset deposits or are interbedded within
328 them and typically occur downdip to the delta foreset deposits (Fig. 4A). Toeset deposits show similar
329 facies to foreset deposits and mainly differ for the bedding dip angle, higher in foreset beds.
330 Conglomerate beds mainly consist of: i) mounded, clast-supported and distribution-type to coarse-tail
331 inverse graded beds (Fig. 4D), with occasional vertical oriented clasts (Fig. 4E); and ii) matrix (sand)
332 supported and crudely normal graded beds. Gravels are moderately to well rounded, with their size
333 ranging from small pebble to large cobble. Angular clasts (i.e., debris) and blocks of cemented
334 sediments have occasionally been found. Clasts are commonly encrusted by oysters and barnacles or

335 bored by *Lithophaga* sp., even if such remains are commonly abraded. Sandstone beds are normally
336 graded, structureless or locally bearing plane-parallel lamination at the top of the beds.

337

338 *Interpretation*

339 The genetic relation with foreset and bottomset deposits, combined with the features of constituent
340 facies, suggests the deposition in delta toset settings of Gilbert-type delta lobes (Colella, 1988;
341 Massari and Colella, 1988; Sohn et al., 1997). In these settings, mounded and clast-supported
342 conglomerate testify the “freezing” of debris flows at the toe of the delta slope (Nemec, 1990; Sohn et
343 al., 1997), whereas matrix-supported conglomerates are attributed to the accumulation of clasts at the
344 toe of the delta slope due to debris fall processes. Sandstone beds were emplaced due to high-density
345 turbidity currents.

346

347 **4.1.7 Foreset deposits of Gilbert-type deltas**

348 *Description*

349 These deposits consist of seaward-inclined (20 to 35°) conglomerate beds and subordinated gravelly
350 sandstone (Fig. 4A, F), vertically stacked up to form thick bodies (up to 60 m), stratigraphically
351 overlying bottomset and toset deposits. The depositional dip of foreset beds typically diminishes
352 downdip and merges with sub-horizontal beds of bottomset and toset facies associations. Locally,
353 however, inclined foreset beds sharply overlie bottomset deposits.

354 Conglomeratic beds are 10 to 100 cm thick (Fig. 4F) and consist of pebble to cobble gravel (with
355 occasional boulders) and include the following facies: i) tabular to lenticular openwork beds, with
356 larger clasts in the downdip part; ii) tabular or mounded beds, matrix (sand) supported and
357 structureless, generally non-graded or occasionally showing coarse-tail inverse grading (Fig. 4F) or
358 shear-banding (Fig. 4G); and iii) tabular, weakly graded and structureless conglomerate beds with

359 erosional bases. Gravel clasts of these facies are frequently bored by *Lithophaga* sp., although these
360 structures are clearly re-worked and abraded. Sandstone beds are composed of coarse-grained sand
361 with scattered gravels, generally cross-stratified upslope or structureless.

362

363 *Interpretation*

364 The overall features of this facies association indicate a deposition in the foreset setting of a Gilbert-
365 type delta (*sensu* Gilbert, 1885; Barrell, 1912; Colella, 1988), where deposition is strongly related to
366 subaqueous sediment-gravity processes connected to collapses of the upper part of the Gilbert-type
367 delta complex (Nemec, 1990). In detail, openwork conglomerate are attributed to debris fall processes,
368 while matrix-supported and mud-free beds are related to cohesionless debris flow processes (*sensu*
369 Nemec and Steel, 1984). Shear bands within these deposits testify syn-depositional internal thrusting
370 due to rapid braking of flows (Massari, 1984; Nemec, 1990; Gobo et al., 2014b). Erosional based beds
371 are the expression of deposition from high-density and turbulent sediment-laden flows (*sensu* Lowe,
372 1982). Sandstone beds deposited due to low-density turbidity currents (*sensu* Lowe, 1982) subjected to
373 a hydraulic jump in delta-slope chutes (Nemec, 1990; Nemec et al., 1999; Gobo et al., 2014a,b).

374

375 **4.1.8 Topset deposits of Gilbert-type deltas**

376 *Description*

377 These deposits are relatively uncommon in the studied area and display a facies assemblage and
378 internal architecture similar to distributary channel deposits. Bedding is sub-horizontal and topset
379 deposits occur directly above the Gilbert-type delta foreset. Toeset sediments are generally coarser
380 grained than the distributary channel deposits.

381

382 *Interpretation*

383 Based on the previously addressed considerations for distributary channel facies association, topset
384 deposits represent the prolongation of river channels within the delta plain that supplies sediments
385 directly to the deltaic system. The stratigraphic position of these deposits above foreset one allow to
386 consider them as the topset deposits (i.e., alluvial distributary plain) of a Gilbert-type delta.

387

388 **4.1.9 Wave-winnowed lag deposits**

389 *Description*

390 These deposits consist of conglomerate with abundant mud-free sandy matrix, forming individual and
391 relatively thin beds (10-50 cm) at the top of the deltaic deposits. Beds are erosionally-based, normally
392 graded and range from sheet-like gravel beds to discontinuous horizons of scattered or clustered gravel
393 clasts. Broken shell remains are common within the sandy matrix and clasts are often encrusted (*Ostrea*
394 *lamellosa*, *Balanus* sp.) and bored by *Lithophaga* sp.

395

396 *Interpretation*

397 The overall features and fossil content indicate deposition as gravel lags originated due to wave-related
398 winnowing processes on the sea-floor (Hwang and Heller, 2002; Cattaneo and Steel, 2003). These
399 processes typically occur during relative sea-level rises and caused the partial erosion of previously
400 deposited sediments, the concentrations of gravel clasts up to form gravel pavements and the removal
401 of fine-grained sediments that are pushed-out in distal position.

402

403 **4.1.10 Slope and Alluvial fan deposits**

404 *Description*

405 These deposits are only exposed in a limited area, limiting their detailed sedimentological investigation
406 (Fig. 5A,B). They consist of poorly sorted pebble to boulder gravels bearing a great amount of

407 interstitial sandy matrix, internally disorganized to crudely normally graded with an a(p) or a(p)a(i)
408 fabric of elongate clasts. Beds are tabular, up to 1m thick and often amalgamated. Clasts are not
409 encrusted or bored by marine organisms.

410

411 *Interpretation*

412 The limited exposures of such deposits prevent a detailed interpretation of the depositional
413 environment. However, the features suggest a deposition due to debris flow processes (Nemec and
414 Steel, 1984) in a sub-aerial environment, possibly connected to an alluvial fan system (Fidolini et al.,
415 2013). This is confirmed by the lack of marine organism traces within these deposits.

416

417 **4.2 Stratigraphic architecture**

418 **4.2.1 Stratigraphic architecture of delta branch 1 (DB1)**

419

420 Investigations on DB1 have been mainly carried out on two outcrops that document the proximal to
421 distal evolution of the deltaic system. Paleocurrent data collected in topset deposits indicate a main
422 WSW transport direction (see rose diagrams in Fig. 5). The landward outcrop is approximately parallel
423 to the main direction of progradation of the deltaic system (Fig. 5), while the basinward outcrop is
424 approximately perpendicular to it (Fig. 6).

425 The DB1 succession starts with shoal-water delta sediments, expressed landwards by fluvial-like
426 distributary channel deposits (Fig. 5A,B), passing basinwards to gently and seaward-inclined mouth-
427 bar deposits. The latter are erosionally overlain in places by gravelly distributary channel sediments
428 (see left corner of Fig. 6A,B). Basinwards, at least two shoal-water elementary deltaic units (hereafter
429 EDUs) displaying a vertical parasequence-like arrangement can be identified. Channel basal scours

430 have a concave-up profile and channels are relatively small in size (1 to 5 m wide and 1-2 m deep, Fig.
431 6B).

432 Shoal-water delta deposition is abruptly interrupted in both outcrops: i) in landward position, the
433 distributary channel sediments are overlain by 3 m thick continental deposits (slope and alluvial fan
434 facies association), overlain in turn by a 50 cm thick sandstone bed pertaining to the wave winnowed
435 lag deposits and by an 8 m thick and poorly exposed bottomset deposits (Fig. 5A,B); ii) basinward
436 (Fig. 6B), shoal-water delta deposits are gently shaped by an erosional surface that marks the base of a
437 thin (50 cm) gravel lag (wave winnowed deposits) above which offshore to prodelta mudstones occur.
438 The surface marked by the base of the wave winnowed lag deposits corresponds to the aforementioned
439 key-surface TS1.

440 Gilbert-type delta deposition starts above TS1 in both the investigated outcrops (Figs. 5A, 6B). In
441 landward position (Fig. 5A), Gilbert-type deposits are mainly expressed by proximal and coarser facies
442 forming m-thick package of sediments characterized by a well-marked coarsening- and shallowing-
443 upward trend, which are bounded by deactivation surfaces. Deactivation surfaces can be interpreted as
444 flooding surfaces *s.s.* when they mark the instauration of marine settings above topset deposits (see Fig.
445 5A,E,F for examples). At a larger scale, EDUs are vertically stacked and display the progressive
446 landward migration of the topset/foreset transition point. The present day erosional relief prevents to
447 observe the topset/foreset transition point of the upper EDU, that however, is characterized by coarser
448 and thicker foreset deposits that spread over older deposits (Fig. 5A). Gilbert-type deposits are abruptly
449 and sharply overlain by a 50 cm thick wave-winnowed lag deposits (Fig. 5A) that, in turn, are overlain
450 by shoal-water delta sandstones (facies associations delta front and mouth-bar, up to 15-20 m in
451 thickness as deducible by the geological map on Fig. 2). The surface marked by the base of these wave-
452 winnowed lag deposits corresponds to the key-surface TS2. Basinwards, Gilbert-type deposition is
453 mainly expressed by proximal to distal facies associations (foreset, toset and bottomset), while topset

454 deposits are absent (Fig. 6A, B). Also in this case, the succession results from the vertical stacking of
455 EDUs, each capped by a flooding/deactivation surface that marks the deactivation of the delta lobe.
456 Lobe deactivation processes are generally sharp, only occasionally gradual as testified by fining-
457 upward trends and the retrogradational attitude of overlying beds. Avulsion processes are locally
458 documented by the lateral emplacement of different deltaic lobes with a “compensational stacking
459 pattern” (i.e., sedimentation in the depression between two lobes). This is particularly evident in the
460 stratigraphically lower Gilbert-type delta lobe, which deposited in the depressed inter-lobe area of the
461 older shoal-water deltaic deposits, onlapping on the inherited morphology (Fig. 6B). At a large scale,
462 the vertical stacking of EDUs displays a progressive increase of fine-grained sediments (bottomset
463 deposits) over coarser sediments (toeset and foreset deposits) towards the upper part of the outcrop.
464 Unfortunately, the upper part of the succession is unexposed preventing the investigation of the entire
465 succession up to the upper shoal-water delta deposits. The overall thickness of Gilbert-type deposits in
466 DB1 is about 65 m.

467

468 **4.2.2 Stratigraphic architecture of delta branch 2 (DB2)**

469

470 Investigations on DB2 have been carried out on several outcrops that well document the proximal (Fig.
471 7) to distal (Fig. 8) evolution of the system. Foreset dips (Figs. 2, 8A) suggest a main NW direction of
472 progradation of the deltaic system. The investigated outcrops are parallel and orthogonal to this
473 direction.

474 Similarly to DB1, deposition in DB2 started with shoal-water delta deposits (Fig. 7A). These deposits
475 are expressed landward generally by coarse-grained distributary channel deposits, with subordinated
476 gravelly sandstone mouth-bar deposits forming m-thick elementary deltaic units that are vertically
477 stacked in a parasequence-like arrangement (Fig. 7A, B). Such deposits pass basinward to gently and

478 seaward-inclined mouth-bar deposits, only locally erosionally overlain by gravelly-rich distributary
479 channel sediments. Distributary channels in DB2 are thicker and wider than those in DB1 (individual
480 channels are up to 5 m high and at least 10-20 m wide). Additionally, these deposits generally comprise
481 coarser sediments than those in DB1 and contain large mud clasts (Fig. 7C), which suggest a greater
482 fluvial energy for the distributive system of the DB2 shoal-water delta.

483 Shoal-water deposition was abruptly replaced by Gilbert-type related deposits through a sharp surface
484 that can be laterally correlated to the aforementioned TS1 surface. Gilbert-type deposition across the
485 entire area starts with bottomset deposits, even if the thickness of these deposits diminishes towards
486 landward positions. In the most landward located outcrops, bottomset deposits are expressed by a thin
487 fine-grained sandstone bed containing remains of marine shells overlying distributary channel
488 sediments (Fig. 7A).

489 Above bottomset deposits, Gilbert-type delta foreset deposits spread over the entire DB2 branch (Figs.
490 7A, 8A) forming a coarse-grained wedge, reaching a maximum thickness of about 50-60 m and
491 bounded at its top by a deactivation surface that marks the end of foreset-related deposition (Fig. 8A).
492 Foreset deposits display a progressive increase in bed inclination, passing from 15-20° in the lower part
493 of the succession up to 28-35° in the upper part (Fig. 8A). Stratigraphic evidence connected to
494 deactivation surfaces can be recognized only at the toe of this coarse-grained wedge (as testified by the
495 superimposition of bottomset deposits above foreset and toeset sediments, Fig. 8A-D), while they are
496 not recognizable in the upper part of the wedge. As a consequence, these Gilbert-type foreset deposits
497 form a single elementary deltaic unit.

498 The deactivation surface at the top of foreset deposits marks the beginning of finer-grained deposition,
499 expressed by the vertically stacking of two EDUs expressed exclusively by bottomset and toeset
500 deposits, forming a thick wedge (left side of the outcrop in Fig. 8A,B). Toeset deposits are
501 characterized by the occurrence of debris and blocks, predominantly made of cemented sandstone (Fig.

502 9A-C) and subordinated cemented conglomerate (Fig. 9A,B,D). Blocks of cemented sandstone contain
503 remains of marine mollusks indicative of a nearshore environment (e.g., *Venus*, *Turritella*, *Chlamis*).
504 The Gilbert-type succession is truncated at its top by a relatively flat erosional surface (corresponding
505 to TS2 surface in DB1, Fig. 8A,B) that marks the base of a 50 cm thick and laterally persistent bed of
506 wave-winnowed lag deposits. Above this bed, sandy shoal-water deposits (facies associations delta
507 front and mouth-bar) occur throughout the investigated area, with average thicknesses ranging between
508 20 and 30 m (Fig. 8A,B).

509

510 **4.2.3 Deposition in intra-branches areas**

511

512 Observations in intra-branches areas (i.e., the area between DB1 and DB2) were made along a small
513 creek incision (see Fig. 2, log 12) where the succession is relatively well exposed (Fig. 10).

514 Sedimentation starts at the base with shoal-water delta mouth-bar deposits abruptly overlain by
515 bottomset deposits via the aforementioned TS1 surface, which is expressed by a 20-30 cm thick gravel
516 lag (wave winnowed lag deposits). Bottomset deposits are only occasionally interbedded with m-thick
517 toeset and foreset sandstone and conglomerate beds (Fig. 10). The ratio between fine-grained and
518 coarse-grained facies is higher than the axial portion of DB1 and DB2 (i.e., fine-grained facies are
519 dominant). At the top of the succession, bottomset deposits are sharply overlain by shoal-water delta
520 front sandstones.

521

522 **5. Discussion**

523

524 The investigated succession documents basal shoal-water delta deposits passing upward to Gilbert-type
525 deposits, in turn overlain by shoal-water delta deposits. Similar stratigraphic organizations are

526 commonly described for active tectonic settings in which the changes in deltaic style are mainly
527 connected to variations in subsidence-related accommodation (Dorsey et al., 1995; García-García et al.,
528 2006; Ghinassi, 2007). In similar settings, thick Gilbert-type deltaic successions are generally
529 connected to stages of rapid subsidence and high sedimentation rates (Dorsey et al., 1995), while thick
530 and vertically stacked shoal water-type deltaic successions typify stages characterized by low to
531 moderate rates of subsidence and low sediment supply (García-García et al., 2006; Ghinassi, 2007).
532 The large-scale stratigraphic architecture of Gilbert-type deltas is strongly influenced by the available
533 accommodation space and the supply of sediments (and their interplay), which are in turn controlled by
534 tectonic and eustasy (cf., Postma 1990a, b; López-Blanco et al., 2000; Marzo and Steel, 2000). The
535 variation of accommodation experienced during the building-up of ancient Gilbert-type deltas can be
536 easily quantified when enough stratigraphic constraints occur. On the contrary, this is generally
537 difficult to estimate in ancient settings. For this reason, its potential role on governing the stratigraphic
538 style of deltas is often neglected and changes in stratigraphic patterns of deltas have been usually
539 interpreted as almost exclusively related to tectonic- and/or climate-related variations in
540 accommodation.

541

542 **6.1 Depositional history of the deltaic complex**

543

544 The large scale stratigraphic architecture of Gilbert-type deposits appears very different in the two
545 investigated branches. In DB1, Gilbert-type deposits result by the vertical stacking of EDUs in an
546 overall retrogradational and aggradational stacking pattern, deducible by: i) the progressive landward
547 migration of the topset/foreset transition point in the landward located outcrop; and ii) the progressive
548 increase of finer-grained and deeper bottomset facies than toset and foreset one towards the upper part
549 of the basinward-located outcrop. In contrast to this generalized retrogradational/aggradational attitude,

550 the younger stratigraphic EDU in the landward-located outcrop (see Fig. 5A) is characterized by the
551 spread of coarse-grained foreset facies over a wide area, suggesting a progradational motif.
552 Unfortunately, the upper part of the basinward-located outcrop is not exposed, therefore preventing the
553 investigation of the seaward stratigraphic counterpart.

554 A different stratigraphic arrangement is observable in DB2. A key feature of the deposits pertaining to
555 this delta branch is the absence of topset deposits above the foreset sediments. The topset deposits are
556 likely to have been completely eroded during the geological events that originated the surface TS2 (i.e.,
557 a base-level drop followed by a ravinement scouring associated with a transgressive event). The lack of
558 topset deposits prevents the identification of the topset/foreset transition point. However, a dominantly
559 progradational/aggradational attitude is suggested by other elements, such as: i) the spreading of foreset
560 deposits over bottomset and toset deposits over a distance of more than 400 m (see Fig. 8A),
561 suggesting a strong progradation of the system; ii) the recognition of deactivation surfaces only at the
562 toe of foresets, indicating a relatively continuous sediment supply that generally typifies the
563 progradational phases; and iii) the progressive increase in bed inclination towards the upper part of the
564 succession, that suggests the progressive increase of available accommodation space over time, as
565 classically expected for aggradational settings.

566 The “wedge” of toset and bottomset deposits that overlie the foreset ones in DB2 indicates that a delta
567 avulsion process occurred. However, toset deposits display a peculiar composition, including blocks
568 of sediments eroded and re-worked by previously deposited nearshore sediments (sandstone blocks
569 with marine fauna, Fig. 9A-C) and foreset deposits (cemented conglomerates, Fig. 9A,B,D). This
570 evidence suggests that the deposition of toset sediments occurred during a base-level drop that led to
571 the subaerial exposure and subsequent erosion of previously deposited sediments. The predominance of
572 blocks eroded by nearshore settings, when compared to those derived by foreset deposits, suggests that
573 erosional processes affected mainly nearshore and topset deposits and only partially Gilbert-type

574 foresets. The stratigraphic position of this “wedge”, just below the surfaces TS2, suggests that these
575 toeset beds could be emplaced during the onset of the base-level drop that originated the composite
576 surface TS2.

577 From a regional point of view, the angular unconformity between coarse-grained and stepped inclined
578 conglomerate and the overlying sub-horizontal sandstone (Fig. 8A,B) has been interpreted by Bonini
579 and Sani (2002) as the expression of an intra-Pliocene tectonic phase that caused the tilting of the basal
580 conglomerate before the deposition of the upper sandstone occurred. This interpretation is not
581 supported by the data presented in this work because: i) the conglomerate dips are comparable with the
582 typical clinostratification expected for foreset deposits of Gilbert-type deltas; ii) the underlying sub-
583 horizontal shoal-water delta deposits document that the succession is not tectonically tilted; and iii) the
584 origin of the aforementioned angular unconformity results from a relative sea-level drop and a
585 subsequent transgression. These considerations allowed to estimate the total accommodation space
586 experienced during the Gilbert-type delta deposition. This is approximately 60-65 m as documented by
587 the thickness of Gilbert-type deposits. Moreover, the thickness of Gilbert-type deposits is comparable
588 in both delta branches, thus indicating that the subsidence acted uniformly in the area, and that the two
589 branches experienced the same amount of accommodation.

590

591 **6.2 Depositional time-framework of DB1 and DB2**

592

593 Deltaic morphodynamic processes (such as deltaic lobe progradation or avulsion) generally acted in
594 rapid time-spans of ten to thousands of years (cf., Wellner et al., 2005; Edmonds et al., 2009; Blum and
595 Roberts, 2012) and this make generally difficult to investigate the depositional time-framework of
596 deltas in ancient settings. The investigated deltaic complex provides helpful data in order to investigate
597 the depositional relationship between the two delta branches:

- 598 • The lower and upper boundaries of the Gilbert-type deposits correspond to two time-equivalent
599 and laterally traceable surfaces (TS1 and TS2, respectively) which act as stratigraphic time-
600 constraints for Gilbert-type delta deposition. Calcareous nannoplankton data provided by
601 Martini et al. (2015) document that in both branches the sediments between TS1 and TS2
602 deposited during in a relatively short time-interval of about 280 Kyr (i.e. within the MNN14/15
603 biozone of nannoplankton biostratigraphy, dated at the time interval 4.13-3.85 Ma according to
604 the biostratigraphic scheme of Rio et al., 1990);
- 605 • Deposition in intra-branches areas is finer-grained than in the axial portion of each delta branch,
606 as typically expected for deposition in the area between two coeval and adjacent deltaic
607 branches;
- 608 • Above TS1, the thickness of fine-grained transgressive deposits is similar in both delta
609 branches, suggesting that coarse-grained Gilbert-type foreset deposition started immediately
610 above the transgressive event in both delta branches. In the case of a diachronous deposition of
611 Gilbert-type foreset deposits in the two delta branches, it would be logical to expect different
612 thicknesses of fine-grained deposits, i.e. thicker in the branch where foreset deposition started
613 later.

614

615 Stratigraphic evidence suggest a coeval deposition in both delta branches. Moreover, an additional
616 indication on this regard is provided by the upper part of the succession, that documents: i) an
617 “anomalous” progradational attitude of the upper EDU in DB1, and ii) evidence of deposition during an
618 overall base-level drop in DB2 (recycled sediments in toset deposits). Since the surface TS2 records
619 an erosional phase which occurred during a relative base-level fall and the following transgression, it
620 would be plausible to consider that the sediments just beneath this surface would have been deposited
621 during the base-level drop. Consequently, the progradational attitude recorded in DB1 and the avulsion

622 process combined with sedimentation of the recycled sediments in DB2 would be connected to the
623 same external controlling factors, i.e. the relative sea-level drop that originated the surface TS2.

624

625 **6.3 Role of sediment supply on the stratigraphic architecture of Gilbert-type deltas**

626

627 The stratigraphic arrangement of deltas (or more in general of siliciclastic sedimentary successions) has
628 been largely governed by the so-called “A/S ratio” (hereafter λ , cf., Jervey, 1988; Muto and Steel,
629 1992, 1997), where “A” indicates the rate of change of accommodation and “S” the rate of sediment
630 supply.

631 Even though the rate of sediment supply deeply influences the arrangement of deltas, a correct
632 evaluation of this parameter is generally possible only in present-day settings (where the amount/type
633 of sediments transported by the distributary system to the delta can be measured) while it is extremely
634 difficult in ancient settings. The role of sediment supply variations on the resulting stratigraphic
635 features of coarse-grained fan-deltas has been addressed by a number of studies (López-Blanco et al.,
636 2000; Marzo and Steel, 2000; López-Blanco, 2006) that have highlighted how the variation in sediment
637 supply over time governs the stratigraphic arrangement of both fundamental transgressive-regressive
638 sequences (i.e., high-frequency) and transgressive-regressive megasequences deposited over a time
639 span of some million years (López-Blanco et al., 2000). Some points remain, however, poorly
640 investigated, for example the stratigraphic arrangement of deltaic systems fed by multiple and coeval
641 fluvial entry points, each providing a different amount of sediments.

642 The deltaic complex analyzed here represents a natural laboratory for testing the role of sediment
643 supply in the stratigraphic architecture of Gilbert-type deltas because: i) the amount of created
644 accommodation is known and it is the same in both delta branches; ii) the coevality of the delta
645 branches ensures that climate-induced base-level fluctuations influenced the delta complex in the same

646 way; and iii) the subsidence acted uniformly in the whole area during deposition. These considerations
647 imply that the rate of change of accommodation (A) can be considered the same in both delta branches
648 (i.e., constant), in turn implying that the only unknown variable for the A/s ratio is the rate of sediment
649 supply (S). Consequently, it can be assumed that the variable “S” is the only responsible for the
650 observed differences in the stratigraphic architecture on the two delta branches.

651 Gilbert-type deposits in DB1 (Figs. 5, 6) are composed of several vertically stacked EDUs showing an
652 overall retrogradational/aggradational stacking pattern in which younger foreset deposits grow on the
653 top of previously deposited topset deposits (Fig. 5A). This stratigraphic organization indicates that the
654 Gilbert-type delta experienced, during its depositional history, the alternation of phases of delta
655 progradation (i.e., $A/s < 1$) and phases characterized by the rapid creation of accommodation space, in
656 which the sediment supply is not enough to counterbalance the generated space ($A/s > 1$). The latter
657 phases are characterized by the drowning of the system and by the inundation of the delta plain (i.e.,
658 topset deposits, see Fig. 11 – Stages 2 and 3). As a consequence, the following new progradation of the
659 deltaic system occurs above the delta plain (Fig. 11 – Stages 4 and 5) and, consequently, the available
660 space for foresets growth corresponds to the water depth between the base-level and the previously
661 deposited delta plain sediments (i.e., topset deposits). If the deltaic progradation exceeds the older
662 topset/foreset brink zone, foreset deposits can advance into deeper water where the total available space
663 results from the underfilled space generated by previously occurred pulses of accommodation
664 generation, as documented by the upper EDU in Figure 5A.

665 A different organization is recognizable in DB2, where the main part of Gilbert-type deposits is
666 expressed by a single EDU characterized by: i) an overall progradational and aggradational attitude; ii)
667 high foresets, up to 60 m in thickness; iii) the progressive increase of delta foreset beds inclination
668 towards the upper part of the succession (Fig. 8A); and iv) the occurrence of deactivation surfaces
669 connected with pulses of increasing in accommodation only at the toe of the delta foresets (Fig. 8A, C).

670 These pieces of evidence suggest that in DB2 the amount of sediment supplied to the river mouth was
671 enough to balance and overcome the pulses of accommodation space creation experienced during the
672 Gilbert-type delta growth, promoting the contemporaneous aggradation and progradation of the system
673 (Fig. 12, Stages 1 to 4).

674 Some stratigraphic features suggest that the difference in sediment supply in the two branches may
675 have been inherited from the older shoal-water deposits. In particular, the thickness and the width of
676 distributary channels of the basal shoal-water delta suggest a more conspicuous sediment supply for
677 DB2, compared to DB1.

678 The presented data highlight that the stratigraphic architecture patterns of Gilbert-type deltas may be
679 dramatically influenced by the amount of sediments delivered at the river mouths or, more in detail, by
680 the capacity of the sediment supply to counteract the pulsating accommodation space generation. As
681 documented, sediment supply variations can drastically change within the same deltaic complex and
682 over short distances.

683

684 **6. Conclusions**

685

686 Large-scale stratigraphic architectures of Gilbert-type deltas have commonly been used as a tool to
687 refine the basin-fill history of coarse-grained and marginal successions. Architectural styles are
688 typically expressed by aggradational, progradational and retrogradational patterns resulting from the
689 interplay between the generated accommodation and the sediment supply experienced during deltas
690 built-up. In ancient settings, however, the quantification of the amount of sediments delivered to the
691 deltaic system is extremely difficult and for this reason many studies frequently neglected this
692 parameter or assumed it constant.

693 This paper provides new insights on the role of sediment supply on the large-scale stratigraphic
694 architecture of Gilbert-type deltas, based on the results of the investigation of a Pliocene deltaic
695 complex composed of two coeval deltaic branches. The two branches experienced the same
696 accommodation space variations during deposition and climate-induced sea-level fluctuations affected
697 the two branches in the same way. The narrowly constrained “accommodation history” provides a rare
698 opportunity to discern the role of sediment supply in the stratigraphic architecture of ancient Gilbert-
699 type deltas.

700 In detail, the deltaic branch characterized by a great sediment supply shows foresets up to 60 m high
701 characterized by a progradational and aggradational trend. Moreover, foreset bed dips display a
702 progressive increase towards the upper part of the succession. Stratigraphic evidence of deactivation
703 surfaces connected to small-scale flooding events or lobes avulsion processes are recognizable only at
704 the toe of the delta body. The overall stratigraphic features indicate that the sediment supply was
705 sufficient to counteract and overcome the accommodation generated during deposition. Conversely, the
706 delta branch that received a minor amount of sediment displays a completely different stratigraphic
707 organization characterized by thin delta foresets (of 2-5 m), vertically stacked to form an aggradational
708 and retrogradational stacking pattern. Such an organization suggests that the sediment supply is not
709 sufficient to counterbalance the accommodation space generated during episodic pulses, forcing the
710 deltaic system to withdraw. The landward retreat of the system implied the inundation of the delta
711 plain, over which new foresets grew and prograded. The available space for foresets growth does not
712 correspond to the basin depth but rather to the depth of water between the base-level and the previously
713 deposited delta plain.

714 This study provides field evidence documenting the role of sediment supply in the large-scale
715 stratigraphic architecture of Gilbert-type deltas, up to generate completely different stratigraphic
716 architectures. The amount of sediment delivered to river mouths can drastically change over short

717 distances (i.e., within the same deltaic complex) and, therefore, caution is necessary when using large-
718 scale stratigraphic architecture of Gilbert-type deltas as a tool to refine the basin-fill history when
719 information about the sediment yields is lacking.

720

721 **Acknowledgements**

722

723 This work is part of the PhD thesis of one of the authors (EA). The research was partially funded by the
724 International Association of Sedimentologists (Postgraduate Grant Scheme -2st session 2014). We are
725 grateful to Francesco Iacoviello (University College London), Massimiliano Ghinassi (University of
726 Padua, Italy) and Katarina Gobo (Statoil ASA, Bergen, Norway) for their constructive comments on a
727 preliminary draft of the manuscript. Two anonymous reviewers and the Associate Editor Jasper Knight
728 made suggestions that greatly improved the manuscript.

729

730 **References**

731

- 732 Aldinucci, M., Ghinassi, M., Sandrelli, F., 2007. Climatic and Tectonic Signature in the Fluvial Infill of
733 a Late Pliocene Valley (Siena Basin, Northern Apennines, Italy). *Journal of Sedimentary Research* 77,
734 398-414.
- 735 Ambrosetti, E., Martini, I., Sandrelli, F., 2017. Shoal-water deltas in high-accommodation settings:
736 Insights from the lacustrine Valimi Formation (Gulf of Corinth, Greece). *Sedimentology*, 64, 425-452.
- 737 Antoni, M., Lazzarotto, A., Costantini, A., Albarello, D., 2005. Quadro conoscitivo, Volume VI, Studi
738 di Geologia. Comune di Pienza, Piano strutturale, 126 pp.
- 739 Arnott, R.W.C., 1995. The Parasequence Definition-Are Transgressive Deposits Inadequately
740 Addressed? *Journal of Sedimentary Research* 65, 1-6.

741 Arragoni, S., Martini, I., Sandrelli, F., 2012. Facies association map of the Pliocene deposits of the
742 central-southern Siena Basin (Tuscany, Italy). *Journal of Maps* 8, 406-412.

743 Backert, N., Ford, M., Malartre, F., 2010. Architecture and sedimentology of the Kerinitis Gilbert-type
744 fan delta, Corinth Rift, Greece. *Sedimentology* 57, 543-586.

745 Barrel, J., 1912. Criteria for the recognition of ancient delta deposits. *Geological Society of America*
746 *Bulletin* 23, 377-446.

747 Bianchi, V., Ghinassi, M., Aldinucci, M., Boscain, N., Martini, I., Moscon, G., Roner, M., 2013.
748 Geological map of Pliocene-Pleistocene deposits of the Ambra and Ombrone valleys (Northern Siena
749 Basin, Tuscany, Italy). *Journal of Maps* 9, 573-583.

750 Bijkerk, J.F., Veen, J.T., Postma, G., Mikeš, D., Strien, W.V., Vries, J.D., 2014. The role of climate
751 variation in delta architecture: lessons from analogue modelling. *Basin Research* 26, 351-368.

752 Blum, M.D., Roberts, H.H., 2012. The Mississippi delta region: past, present, and future. *Annual*
753 *Review of Earth and Planetary Sciences* 40, 655-683.

754 Bonini, M., Sani, F., 2002. Extension and compression in the Northern Apennines (Italy) hinterland:
755 Evidence from the late Miocene-Pliocene Siena-Radicofani Basin and relations with basement
756 structures. *Tectonics* 21, 1-35.

757 Bossio, A., Cerri, R., Costantini, A., Gandin, A., Lazzarotto, A., Magi, M., Mazzanti, R., Mazzei, R.,
758 Sagri, M., Salvatorini, G., Sandrelli, F., 1992. I Bacini distensivi Neogenici e Quaternari della Toscana.
759 In: 76a Riunione Estiva SGI-Convegno SIMP, Guida all'escursione, B4, Società Geologica Italiana,
760 pp. 198-227.

761 Bossio, A., Costantini, A., Lazzarotto, A., Liotta, D., Mazzanti, R., Salvatorini, G., Sandrelli, F., 1993.
762 Rassegna delle conoscenze sulla stratigrafia del Neoauctono toscano. *Memorie della Società*
763 *Geologica Italiana* 49, 17-98.

764 Bridge, J.S., 2003. Rivers and floodplains. Forms, processes and sedimentary record. Blackwell,
765 Oxford, 491 pp.

766 Brogi, A., 2011. Bowl-shaped basin related to low-angle detachment during continental extension: The
767 case of the controversial Neogene Siena Basin (central Italy, Northern Apennines). *Tectonophysics*
768 499, 54-76.

769 Brogi, A., Capezzuoli, E., Martini, I., Picozzi, M., Sandrelli, F., 2014. Late Quaternary tectonics in the
770 inner Northern Apennines (Siena Basin, southern Tuscany, Italy) and seismotectonic implication.
771 *Journal of Geodynamics* 76, 25-45.

772 Brunet, C., Monié, P., Jolivet, L., Cadet, J.P., 2000. Migration of compression and extension in the
773 Tyrrhenian Sea, insights from $^{40}\text{Ar}/^{39}\text{Ar}$ ages on micas along a transect from Corsica to Tuscany.
774 *Tectonophysics* 321, 127-155.

775 Carmignani, L., Decandia, F.A., Disperati, L., Fantozzi, P.L., Lazzarotto, A., Liotta, D., Oggiano, G.,
776 1995. Relationships between the Tertiary structural evolution of the Sardinia-Corsica-Provençal
777 Domain and the Northern Apennines. *Terra Nova* 7, 128-137.

778 Carmignani, L., Decandia, F.A., Disperati, L., Fantozzi, P.L., Kligfield, R., Lazzarotto, A., Liotta, D.,
779 Meccheri, M., 2001. Inner Northern Apennines. In: Vai, G.B., Martini, I.P. (Eds.), *Anatomy of an*
780 *Oroge. The Apennines and Adjacent Mediterranean Basins*. Kluwer Academic Publishers, Dordrecht
781 pp. 197-214.

782 Carvajal, C., Steel, R., Petter, A., 2009. Sediment supply: The main driver of shelf-margin growth.
783 *Earth-Science Reviews*, 96, 221-248.

784 Catuneanu, O., 2002. Sequence stratigraphy of clastic systems: concepts, merits, and pitfalls. *Journal of*
785 *African Earth Science* 35, 1-43.

786 Cattaneo, A., Steel, R.J., 2003. Transgressive deposits: a review of their variability. *Earth-Science*
787 *Reviews* 62, 187-228.

788 Coe, A.L., Bosence, D.W.J., Church, K.D., Flint, S.S., Howell, J.A., Wilson C.R., 2002. The
789 Sedimentary Record of Sea Level Change. Cambridge University Press, Cambridge, 288 pp.

790 Colella, A., 1988. Fault-controlled marine Gilbert-type fan deltas. *Geology* 16, 1031-1034.

791 Collinson, J.C., Mountney, N.P., Thompson, D.B., 2006. *Sedimentary Structures*. Terra Publications,
792 Harpenden, England, 292 pp.

793 Costantini, A., Decandia, F.A., Lazzarotto, A., Liotta, D., Mazzei, R., Pascucci, V., Salvatorini, G.,
794 Sandrelli, F., 2009. Carta Geologica d'Italia alla Scala 1:50.000, Foglio 296-Siena. Tipografia A.T.I.,
795 APAT-Roma, 129 pp.

796 Dorsey, R.J., Umhoefer, P.J., Renne, P.R., 1995. Rapid subsidence and stacked Gilbert-type fan deltas,
797 Pliocene Loreto basin, Baja California Sur, Mexico. *Sedimentary Geology* 98, 181-204.

798 Edmonds, D.A., Hoyal, D.C., Sheets, B.A., Slingerland, R.L., 2009. Predicting delta avulsions:
799 Implications for coastal wetland restoration. *Geology* 37, 759-762.

800 Ethridge, F.G., Wescott, W.A., 1984. Tectonic setting, recognition and hydrocarbon reservoir potential
801 of fan-delta deposits. In: Koster, E.H., Steel, R.J. (Eds), *Sedimentology of gravels and conglomerates*.
802 Canadian Society of Petroleum Geologists, Memoir 10, pp. 217-235.

803 Fidolini, F., Ghinassi, M., Aldinucci, M., Billi, P., Boaga, J., Deiana, R., Brivio, L., 2013. Fault-
804 sourced alluvial fans and their interaction with axial fluvial drainage: An example from the Plio-
805 Pleistocene Upper Valdarno Basin (Tuscany, Italy). *Sedimentary Geology* 289, 19-39.

806 Finetti, I.R., Boccaletti, M., Bonini, M., Del Ben, A., Geletti, R., Pipan, M., Sani, F., 2001. Crustal
807 section based on CROP seismic data across the North Tyrrhenian-Northern Apennines-Adriatic Sea.
808 *Tectonophysics* 343, 135-163.

809 García-García, F., Fernández, J., Viseras, C., Soria, J.M., 2006. Architecture and sedimentary facies
810 evolution in a delta stack controlled by fault growth (Betic Cordillera, southern Spain, late Tortonian).
811 *Sedimentary Geology* 185, 79-92.

812 Ghinassi, M., 2007. The effects of differential subsidence and coastal topography on high-order
813 transgressive–regressive cycles: Pliocene nearshore deposits of the Val d'Orcia Basin, Northern
814 Apennines, Italy. *Sedimentary Geology* 202, 677-701.

815 Gilbert, G.K., 1885. The topographic features of lake shores. U.S. Geological Survey Annual Report
816 No. 5, 75-123.

817 Gobo, K., Ghinassi, M., Nemec, W., Sjursen, E., 2014a. Development of an incised valley-fill at an
818 evolving rift margin: Pleistocene eustasy and tectonics on the southern side of the Gulf of Corinth,
819 Greece. *Sedimentology* 61, 1086-1119.

820 Gobo, K., Ghinassi, M., Nemec, W., 2014b. Reciprocal changes in foreset to bottomset facies in a
821 Gilbert-type delta: response to short-term changes in base level. *Journal of Sedimentary Research* 84,
822 1079–1095.

823 Haq, B.U., Hardenbol, J., Vail, P.R., 1987. Chronology of fluctuating sea levels since the Triassic.
824 *Science* 235, 1156-1167.

825 Harms, J.C., Southard, J.B., Spearing, D.R., Walker, R.G., 1975. Depositional environments as
826 interpreted from Primary Sedimentary Structures and Stratification Sequences. SEPM, Short Course
827 Notes #2, Tulsa, OK, 153 pp.

828 Harms, J.C., Southard, J.B., Walker, R.G., 1982. Structures and Sequences in Clastic Rocks. SEPM
829 Short Course No. 9, Lecture Note. Society of Economic Paleontologists and Mineralogists, Tulsa, OK.

830 Helland-Hansen, W., Martinsen, O.J., 1996. Shoreline trajectories and sequences: description of
831 variable depositional-dip scenarios. *Journal of Sedimentary Research* 66, 670-688.

832 Hwang, I.G., Heller, P.L., 2002. Anatomy of a transgressive lag: Panther Tongue Sandstone, Star Point
833 Formation, central Utah. *Sedimentology* 49, 977-999.

834 Jervey, M.T., 1988. Quantitative geological modeling of siliciclastic rock sequences and their seismic
835 expression. In: Wilgus, C.K., Hastings, B.S., Kendall, C.G.St.C., Posamentier, C.A., Ross, C.A., Van

836 Wagoner, J.C. (Eds.), *Sea-Level Changes: An Integrated Approach*. Special Publication of the Society
837 of Economic Paleontologist and Mineralogist 42, pp. 47–69.

838 Jolivet, L., Faccenna, C., Goffè, B., Mattei, M., Rossetti, F., Brunet, C., Storti, F., Funiciello, R.,
839 Cadet, J.P., D'Aagostino, N., Parra, T., 1998. Midcrustal shear zones in postorogenic extension:
840 Example from the northern Tyrrhenian Sea. *Journal of Geophysical Research* 103, 12,123–12,160.

841 Johnson, H.D., Baldwin, C.T., 1996. Shallow clastic sea. In: Reading, H.G. (Ed.), *Sedimentary*
842 *environments: Processes, Facies and Stratigraphy*. Blackwell Science, 3rd edition, Oxford, pp. 232-280.

843 Li, Y., Bhattacharya, J., 2014. Facies architecture of asymmetrical branching distributary channels:
844 Cretaceous Ferron Sandstone, Utah, USA. *Sedimentology* 61, 1452-1483.

845 Liotta, D., Salvatorini, G., 1994. Evoluzione sedimentaria e tettonica della parte centro-meridionale del
846 bacino pliocenico di Radicofani. *Studi Geologici Camerti, Volume Speciale 1*, 65-77.

847 Leren, B.L., Howell, J., Enge, H., Martinius, A.W., 2010. Controls on stratigraphic architecture in
848 contemporaneous delta systems from the Eocene Roda Sandstone, Tremp-Graus Basin, northern Spain.
849 *Sedimentary Geology* 229, 9-40.

850 López-Blanco, M., Marzo, M., Piña, J., 2000. Transgressive–regressive sequence hierarchy of foreland,
851 fan-delta clastic wedges (Montserrat and Sant Llorenç del Munt, Middle Eocene, Ebro Basin, NE
852 Spain). *Sedimentary Geology* 138, 41-69.

853 López-Blanco, M., 2006. Stratigraphic and tectonosedimentary development of the Eocene Sant
854 Llorenç del Munt and Montserrat fan-delta complexes (Southeast Ebro basin margin, Northeast Spain).
855 *Contributions to Science*, 3, 125-148.

856 Lowe, D.R., 1982. Sediment gravity flows: II Depositional models with special reference to the
857 deposits of high-density turbidity currents. *Journal of Sedimentary Research* 52, 279-297.

858 Manganelli, G., Martini, I., Benocci, A., 2011. A new *Janulus* species (Gastropoda, Pulmonata,
859 Gastrodontidae) from the Zanclean (early Pliocene) of Tuscany (central Italy). *Bollettino della Società*
860 *Paleontologica Italiana* 50, 165-173.

861 Manganelli, G., Spadini, V., Martini, I., 2010. Rediscovery of an enigmatic Euro-Mediterranean
862 Pliocene nassariid species: *Nassarius crassiusculus* Bellardi, 1882 (Gastropoda: Nassariidae).
863 *Bollettino della Società Paleontologica Italiana* 49, 195-202.

864 Marinelli, G., 1975. Magma evolution in Italy. In: Squyres, C.H. (Ed.), *Geology of Italy. The Earth*
865 *Soc. of the Libyan Arab Republic, Tripoli*, pp. 165-219.

866 Marini, L., 2001. *Stratigrafia delle Formazioni Plioceniche nell'area a Nord di Pienza (Siena)*. Master
867 Degree Thesis, University of Siena, 86 pp.

868 Martini, I., Aldinucci, M., Foresi, L.M., Mazzei, R., Sandrelli, F., 2011. Geological map of the Pliocene
869 succession of the Northern Siena Basin (Tuscany, Italy). *Journal of Maps* v2011, 193-205.

870 Martini, I., Arragoni, S., Aldinucci, M., Foresi, L.M., Bambini, A.M., Sandrelli, F., 2013. Detection of
871 detached forced-regressive nearshore wedges: a case study from the central-southern Siena Basin
872 (Northern Apennines, Italy). *International Journal of Earth Sciences* 102, 1467-1489.

873 Martini, I., Ambrosetti, E., Foresi, L.M., Bambini, A.M., Sandrelli, F., 2015. Stratigraphic architecture
874 of a supply-dominated Gilbert-type delta in a tectonically active basin (Pliocene Siena Basin, Italy). In:
875 Costamagna, L.G., Andreucci, S. (Eds.), *Abstract Book of the XII Congresso Geosed*, 21-27 Sept.
876 2015, Cagliari, pp. 51-53.

877 Martini I., Sandrelli F., 2015. Facies analysis of a Pliocene river-dominated deltaic succession (Siena
878 Basin, Italy): Implications for the formation and infilling of terminal distributary channels.
879 *Sedimentology* 62, 234-265.

880 Martini, I., Foresi, L.M., Bambini, A.M., Riforgiato, F., Ambrosetti, E. and Sandrelli, F., 2016.
881 *Calcareous plankton bio-chronostratigraphy and sedimentology of the "I Sodi" section (Siena Basin,*

882 Italy): a key section for the uppermost Neogene marine deposition in the inner northern Apennines.
883 Italian Journal of Geosciences 135, 540-547.

884 Martini, I.P., Sagri, M., 1993. Tectono-sedimentary characteristics of Late Miocene-Quaternary
885 extensional basins of the Northern Apennines, Italy. Earth-Science Reviews, 34, 197-233.

886 Marzo, M., Steel, R.J., 2000. Unusual features of sediment supply-dominated, transgressive–regressive
887 sequences: Paleogene clastic wedges, SE Pyrenean foreland basin, Spain. Sedimentary Geology 138, 3-
888 15.

889 Massari, F., 1984. Resedimented conglomerates of a Miocene fan-delta complex, Southern Alps, Italy.
890 In: Koster, E.H., Steel, R.J. (Eds.), Sedimentology of Gravels and Conglomerates, Memoir of the
891 Canadian Society of Petroleum Geology 10, pp. 259–278.

892 Massari, F., Colella, A., 1988. Evolution and types of fan-delta systems in some major tectonic
893 settings. In: Nemeč, W., Steel, R.J. (Eds.), Fan deltas: Sedimentology and tectonic settings, pp. 103-
894 122.

895 Miller, K.G., Kominz, M.A., Browning, J.V., Wright, J.D., Mountain, G.S., Katz, M.E., Sugarman,
896 P.J., Cramer, B.S., Christie-Blick, N., Pekar, S.F., 2005. The Phanerozoic record of global sea-level
897 change. Science 310, 1293-1298.

898 Mortimer, E., Gupta, S., Cowie, P., 2005. Clinoform nucleation and growth in coarse-grained deltas,
899 Loreto basin, Baja California Sur, Mexico: a response to episodic accelerations in fault displacement.
900 Basin Research 17, 337–359.

901 Mulder, T., Alexander, J., 2001. The physical character of subaqueous sedimentary density flow and
902 their deposits. Sedimentology 48, 269-299.

903 Mulder, T., Syvitski, J.P.M., Migeon, S., Faugères, J.-C., Savoye, B., 2003. Marine hyperpycnal flows:
904 initiation, behavior and related deposits. A review. Marine and Petroleum Geology 20, 861-882.

905 Muto, T., Steel, R.J., 1992. Retreat of the front in a prograding delta. Geology 20, 967-970.

906 Muto, T., Steel, R.J., 1997. Principles of regression and transgression: the nature of the interplay
907 between accommodation and sediment supply: perspectives. *Journal of Sedimentary Research* 67, 994-
908 1000.

909 Nemec, W., Steel, R.J., 1984. Alluvial and coastal conglomerates: their significant features and some
910 comments on gravelly mass-flow deposits. In: Koster, E.H., Steel, R.J. (Eds.), *Sedimentology of*
911 *Gravels and Conglomerates*, Memoir of the Canadian Society of Petroleum Geology 10, pp. 1-31.

912 Nemec, W., Steel, R.J., 1988. What is a fan delta and how do we recognize it. In: Nemec, W., Steel,
913 R.J. (Eds.), *Fan Deltas: sedimentology and tectonic settings*. Blackie and Son, London, pp. 3-13.

914 Nemec, W., 1990. Aspects of sediment movement on steep delta slopes. In: Colella, A., Prior, D.B.
915 (Eds.), *Coarse-grained deltas*, Blackwell Publishing Ltd., Oxford, pp. 29-73.

916 Nemec, W., 1995. The dynamics of deltaic suspension plumes. In: Oti, M.N., Postma, G. (Eds.),
917 *Geology of deltas*. Balkema, Rotterdam, pp. 31-93.

918 Nemec, W., Lønne, I.D.A., Blikra, L.H., 1999. The Kregnes moraine in Gauldalen, west-central
919 Norway: anatomy of a Younger Dryas proglacial delta in a palaeofjord basin. *Boreas* 28, 454-476.

920 Olariu, C., Steel, R.J., Petter, A.L., 2010. Delta-front hyperpycnal bed geometry and implications for
921 reservoir modeling: Cretaceous Panther Tongue delta, Book Cliffs, Utah. *AAPG Bulletin* 94, 819-845.

922 Pascucci, V., Merlini, S., Martini, I.P., 1999. Seismic stratigraphy of the Miocene-Pleistocene
923 sedimentary basins of the Northern Tyrrhenian Sea and Western Tuscany (Italy). *Basin Research* 11,
924 337-356.

925 Petter, A.L., Steel, R.J., 2006. Hyperpycnal flow variability and slope organization on an Eocene shelf
926 margin, Central Basin, Spitsbergen. *AAPG Bulletin* 90, 1451-1472.

927 Plink-Björklund, P., Steel, R.J., 2004. Initiation of turbidity currents: outcrop evidence for Eocene
928 hyperpycnal flow turbidites. *Sedimentary Geology* 165, 29-52.

929 Posamentier, H.W., Allen, G.P., 1993. Variability of the sequence stratigraphic model: effects of local
930 basin factors. *Sedimentary Geology* 86, 91-109.

931 Posamentier, H.W., Allen, G.P., 1999. Siliciclastic sequence stratigraphy; sequence stratigraphy:
932 concepts and applications. *SEPM Concepts in Sedimentology and Paleontology* no. 7, 210 pp.

933 Postma, G., Roep, T.B., 1985. Resedimented conglomerates in the bottomsets of Gilbert-type gravel
934 deltas. *Journal of Sedimentary Research* 55, 874-885.

935 Postma, G., 1990a. An analysis of the variation in delta architecture. *Terra Nova* 2, 124-130.

936 Postma, G., 1990b. Depositional architecture and facies of river and fan deltas: A synthesis. In: Colella,
937 A., Prior, D.B. (Eds.), *Coarse-grained deltas*. Blackwell Publishing Ltd., Oxford, UK, pp. 13-27.

938 Postma, G., 1995. Sea-level-related architectural trends in coarse-grained delta complexes.
939 *Sedimentary Geology* 98, 3-12.

940 Rio D., Raffi I., Villa G., 1990. Pliocene-Pleistocene calcareous nannofossils distribution patterns in
941 the western Mediterranean. *Proceedings of the Ocean Drilling Program, Scientific Results* 107, 513–
942 533.

943 Schumm, S.A., Lichty, R.W., 1965. Time, space, and causality in geomorphology. *American Journal of*
944 *Science* 263, 110-119.

945 Smith, N.D., 1974. Sedimentology and bar formation in the upper Kicking Horse River, a braided
946 outwash stream. *The Journal of Geology* 82, 205-223.

947 Sohn, Y.K., Kim, S.B., Hwang, I.G., Bahk, J.J., Choe, M.Y., Chough, S.K., 1997. Characteristics and
948 depositional processes of large-scale gravelly Gilbert-type foresets in the Miocene Doumsan fan delta,
949 Pohang Basin, SE Korea. *Journal of Sedimentary Research* 67, 130-141.

950 Van Wagoner, J.C., Posamentier, H.W., Mitchum, R.M., Vail, P.R., Sarg, J.F., Loutit, T.S., Hardenbol,
951 J., 1988. An overview of sequence stratigraphy and key definitions. In: Wilgus, C.K., Hastings, B.S.,

952 Kendall, C.G.St.C., Posamentier, H.W., Ross, C.A., Van Wagoner, J.C. (Eds.), Sea Level Changes—
953 An Integrated Approach. SEPM Special Publication 42, pp. 39–45.

954 Van Wagoner, J.C., Mitchum, R.M., Campion, K.M., Rahmanian, V.D., 1990. Siliciclastic sequence
955 stratigraphy in well logs, cores, and outcrops: Concepts for high-resolution correlation of time and
956 facies, AAPG Methods in Exploration Series 7, 55 pp.

957 Walker, R.G., James, N.P., 1992. Facies, facies models and modern stratigraphic concepts. In: Walker,
958 R.G., James, N.P. (Eds), Facies Models - Response to Sea Level Change. Geological Association of
959 Canada, St. John's, pp. 1-14.

960 Wellner, R., Beaubouef, R., Van Wagoner, J.C., Roberts, H., Sun, T., 2005. Jet plume depositional
961 bodies-the primary building blocks of Wax Lake Delta. Gulf Coast Association of Geological
962 Societies, Transactions 55, 867-909.

963

964 **Figure Captions**

965

966 **Fig. 1.** (A) Tectonic sketch of the Northern Apennines. (B) Simplified geological map of the Siena
967 Basin (after Bossio et al. 1992, 1993 and Brogi, 2011). (C) Synthetic stratigraphic columns of the
968 Pliocene sedimentary infill in various sectors of the Siena-Radicofani basins and their bio- and chrono-
969 stratigraphic correlation (data for the Siena sub-basin derived from Bossio et al., 1992, 1993; Martini
970 and Sandrelli, 2015; Martini et al., 2015; data for the Radicofani sub-basin derived from Liotta and
971 Salvatorini, 1994).

972 **Fig. 2.** Geological map of the investigated area with locations of measured sections.

973 **Fig. 3.** Main features of shoal-water delta deposits. (A) Slight-lobate and poorly sorted sandstone,
974 organized in coarsening-upward lithosomes that typifies delta front deposits (woman for scale is *ca.*

975 170 cm tall). (B) Pen shells in life position, associated to other shell fragments, within delta front
976 deposits (cap lens is 5.5 cm in diameter). Shell-rich beds are associated with sediment starvation
977 settings connected to flooding surfaces and/or delta lobes avulsion processes. (C) Coarsening-upward
978 and slight lobate gravelly sandstone of mouth-bar facies association, erosionally overlain by fining-
979 upward sandy conglomerate of distributary channel facies association.

980

981 **Fig. 4.** Main features of Gilbert-type delta deposits. (A) Stratigraphic relationship between bottomset,
982 toeset and foreset deposits (man for scale is *ca.* 180 cm tall). (B-C) Isolated clasts within sandstone and
983 sandy mudstone beds of bottomset facies association. (D) Distribution-type inverse graded and sub-
984 horizontal conglomerate bed that typifies toeset deposits. (E) Conglomerate bed (toeset facies
985 association) characterized by abundant sandy matrix and vertically aligned long clasts, interbedded
986 with sandy bottomset deposits (metre stick for scale is 10 cm long). (F) Vertically stacked
987 conglomerate beds of foreset facies association. (G) Shear-bands within a conglomerate bed of foreset
988 deposits (encircled hammer for scale is 28.5 cm long).

989

990 **Fig. 5.** Stratigraphic architecture of delta branch 1, landward located outcrop: (A) Line-drawing
991 (vertical scale = horizontal scale), sedimentological logs and palaeocurrent data of the investigated
992 outcrop. Note the overall retrogradational/aggradational attitude of Gilbert-type deposits, marked by
993 the landward migration of the topset/foreset transition point. Main features are detailed in the following
994 figures. (B) Basal part of the outcrop where the basal distributary channel deposits are abruptly overlain
995 by slope and alluvial fan deposits (man for scale is 1.80 cm tall). (C) Sub-horizontal sandy
996 conglomerate of topset facies association overlain by foreset deposits through an intervening flooding
997 surface. (D) Sandy foreset deposits exposed in the basinward part of the outcrop. (E-F) Close-up view

998 of a mudstone bed (bottomset facies association) marking a transgressive event and indicating a
999 temporary starving of coarse-grained sediments.

1000

1001 **Fig. 6.** Stratigraphic architecture of delta branch 1, basinward located outcrop: (A) Picture of the
1002 investigated cliff with location of log traces. (B) Line-drawing and sedimentological log of the outcrop
1003 in Fig. 6A (vertical scale = horizontal scale). Note the overall retrogradational/aggradational attitude of
1004 Gilbert-type deposits, marked by the progressive increase of fine-grained facies toward the upper part
1005 of the outcrop.

1006

1007 **Fig. 7.** Stratigraphic architecture of delta branch 2, landward located outcrop. (A) Line-drawing of the
1008 investigated outcrop (see Fig. 2 for location). Vertical scale = horizontal scale. Surface TS1 marks the
1009 transition between the basal shoal-water delta deposits and the Gilbert-type delta related sediments. (B)
1010 Close-up view of the stratigraphic relationship between mouth-bar and distributary channel deposits of
1011 the basal shoal-water delta. Man for scale (encircled) is 1.80 m tall. (C) Close-up view of a large mud
1012 clast within distributary channel deposits (woman for scale is 1.65 m tall).

1013

1014 **Fig. 8.** (A) Correlation panel showing the stratigraphic evolution and architecture of delta branch 2. (B)
1015 Basinward located outcrop where it is possible to observe the upper part of the succession (the lower
1016 shoal-water delta deposits are shown on Fig. 7). Note the progradational attitude of foreset deposits.
1017 Local deactivations are evidenced only at the toe of the delta lobe by the superimposition of
1018 bottomset/toeset deposits above foreset deposits. (C) Detail of the facies association transition
1019 occurring at the toe of the Gilbert-type foreset. (D) Close-up view of the transition between foreset and
1020 bottomset deposits.

1021

1022 **Fig. 9.** (A) Enlargement of the basal portion of log “9” of Figure 8A. Note the occurrence of recycled
1023 sediments expressed by blocks of cemented sandstone and conglomerate. (B-C-D) Field expression of
1024 toeset deposits containing blocks of cemented sandstone (encircled by a yellow solid line) and
1025 conglomerate (encircled by an orange solid line). The sandstone blocks contain shell remains indicative
1026 of a nearshore environment, while the blocks of cemented conglomerate show sedimentological
1027 features similar to those of the foreset deposits. Hammer for scale is 28.5 cm long.

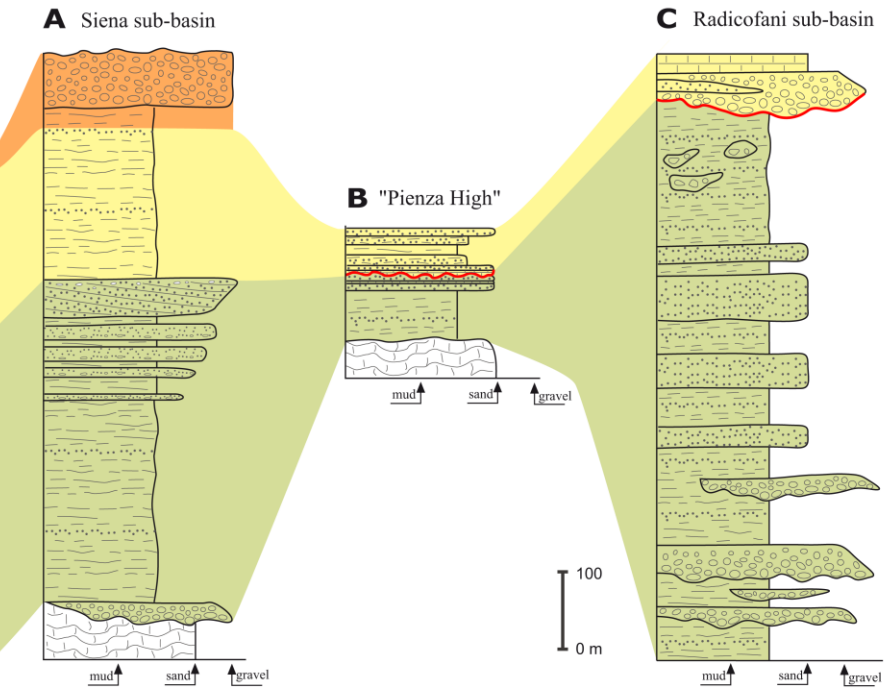
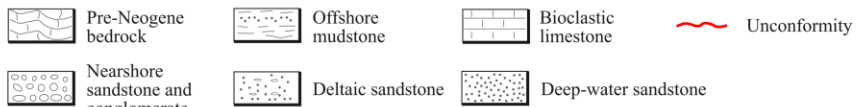
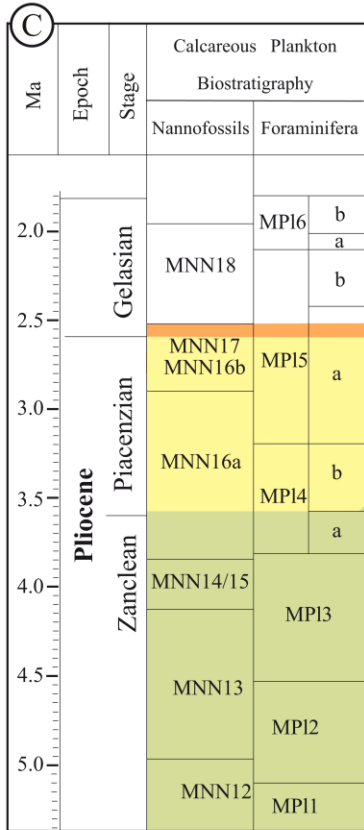
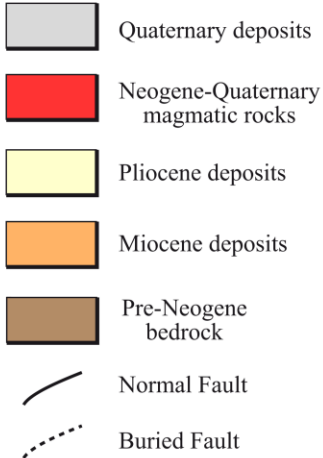
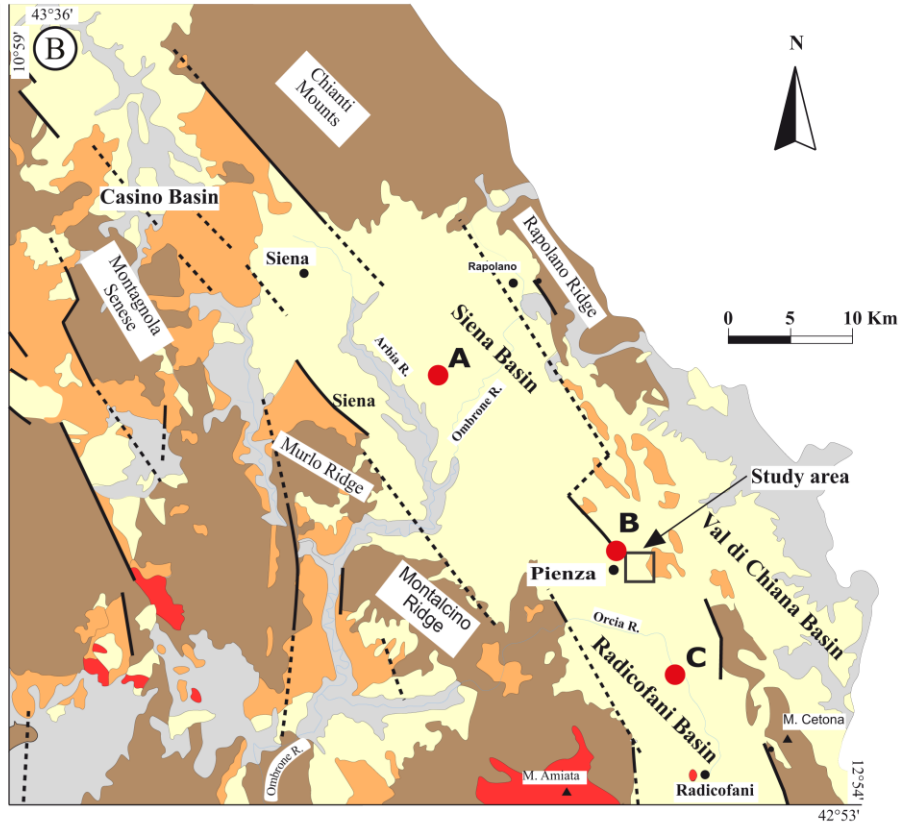
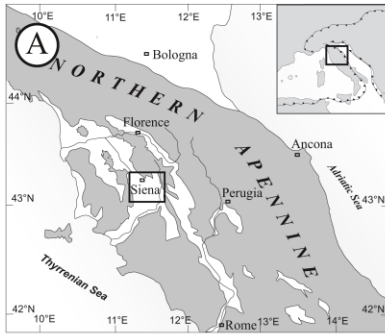
1028
1029 **Fig. 10.** Sedimentary log collected between the two branches. See Figure 2 for location of log.

1030
1031 **Fig. 11.** Depositional model for Gilbert-type deltas developed in settings characterized by a relatively
1032 low sediment supply and pulsating accommodation creation. Model is derived by data collected in
1033 DB1.

1034
1035 **Fig. 12.** Depositional model for Gilbert-type deltas developed in settings characterized by a relatively
1036 high sediment supply and pulsating accommodation creation. Model is derived by data collected in
1037 DB2.

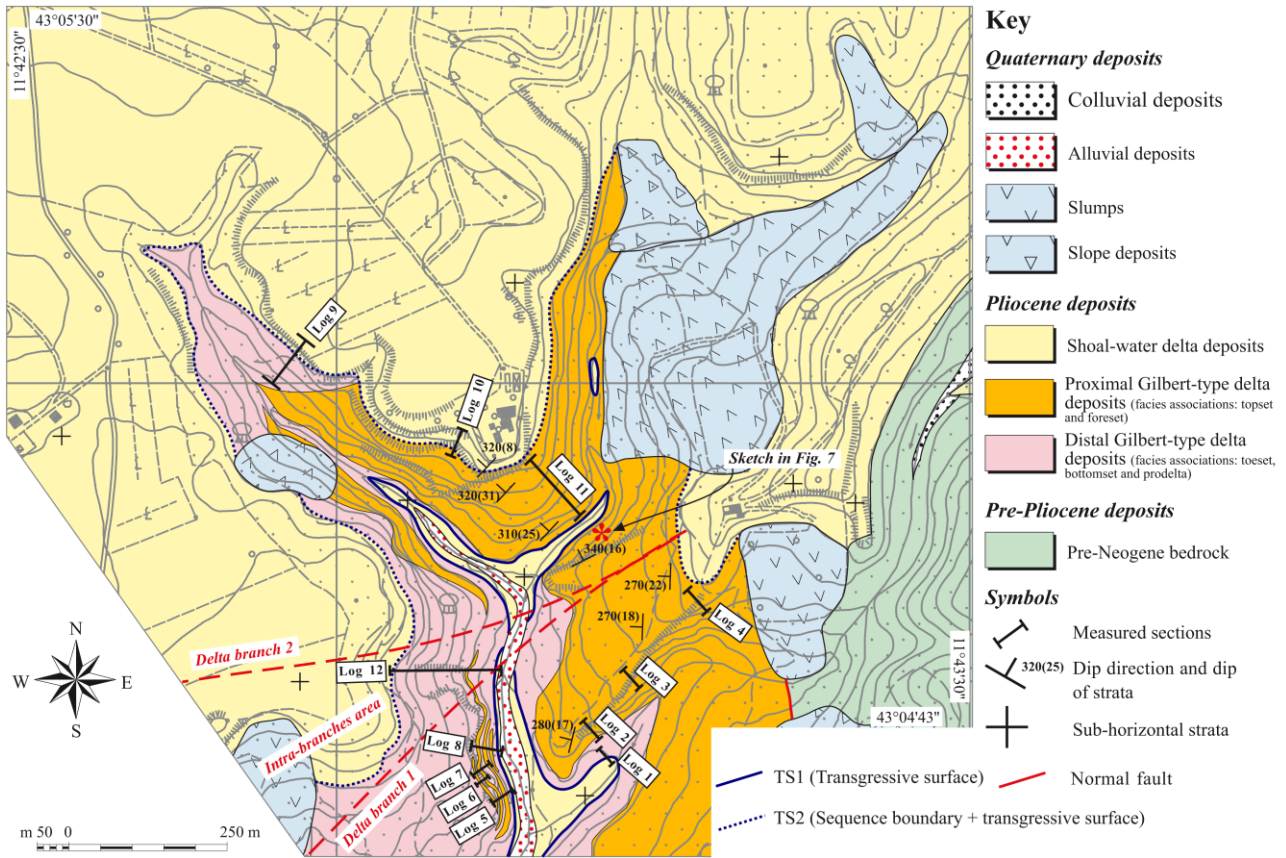
1038
1039 **Table 1.** Summary of main features in the recognized facies associations.

1040



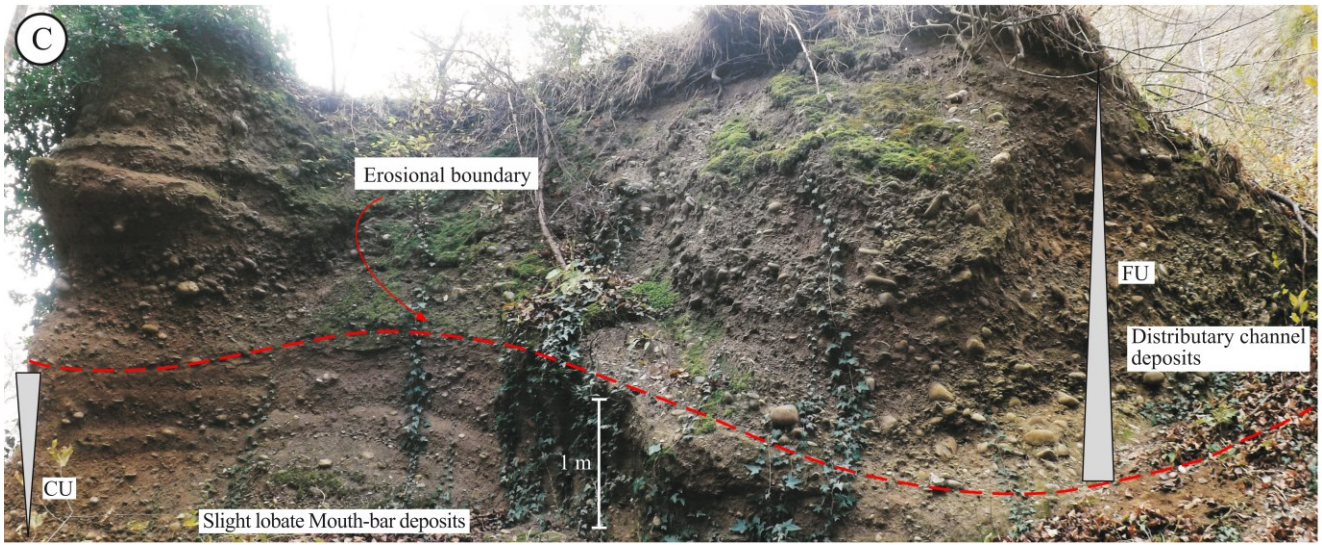
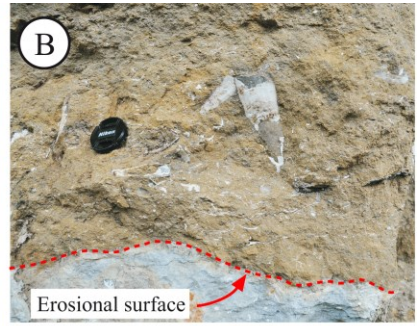
1041

1042



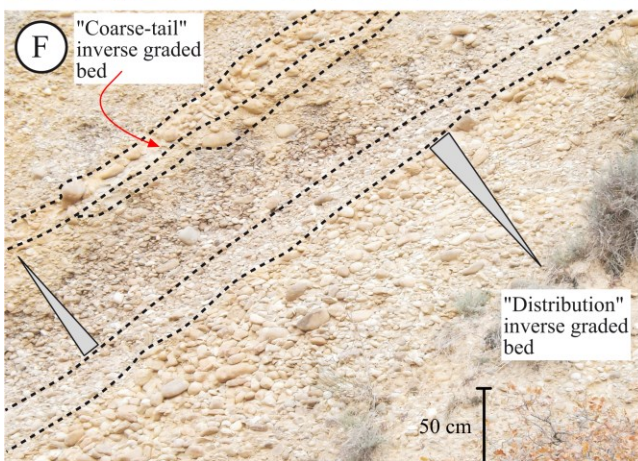
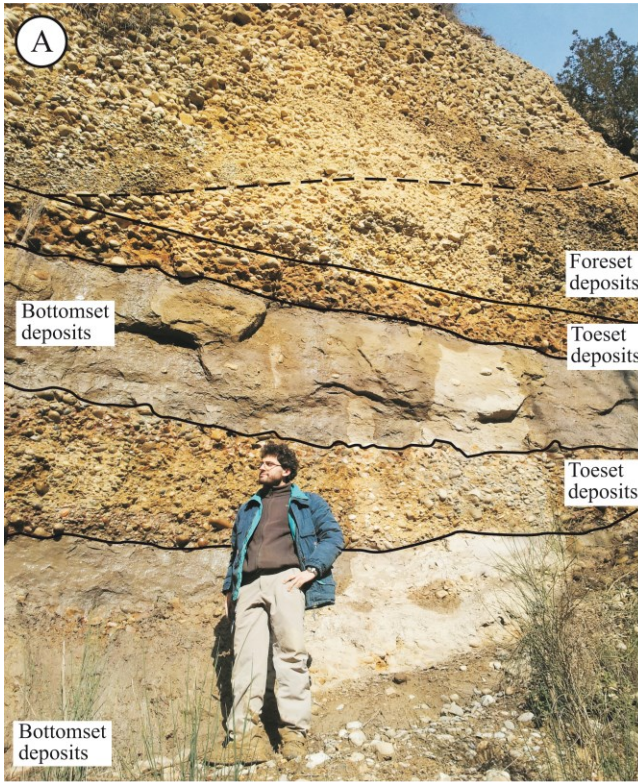
1043

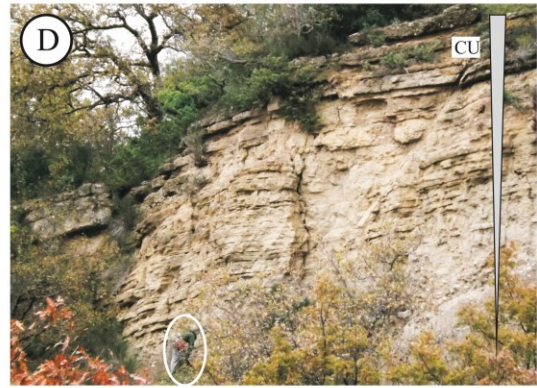
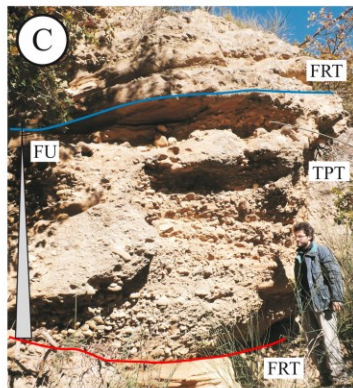
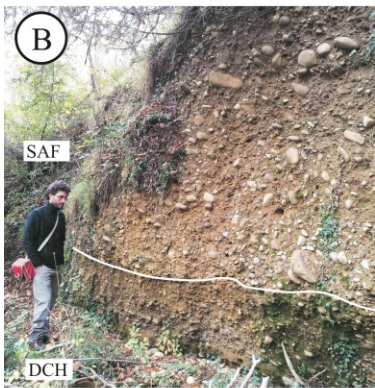
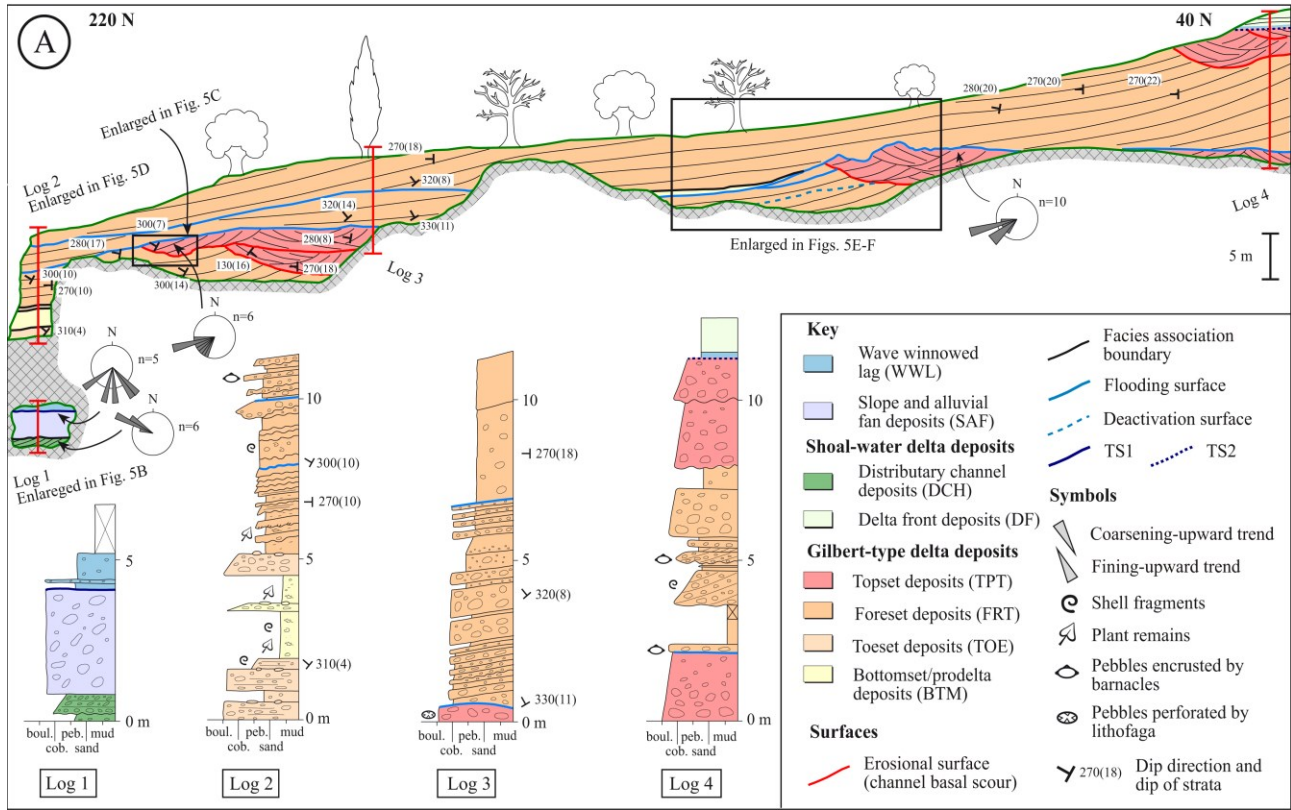
1044

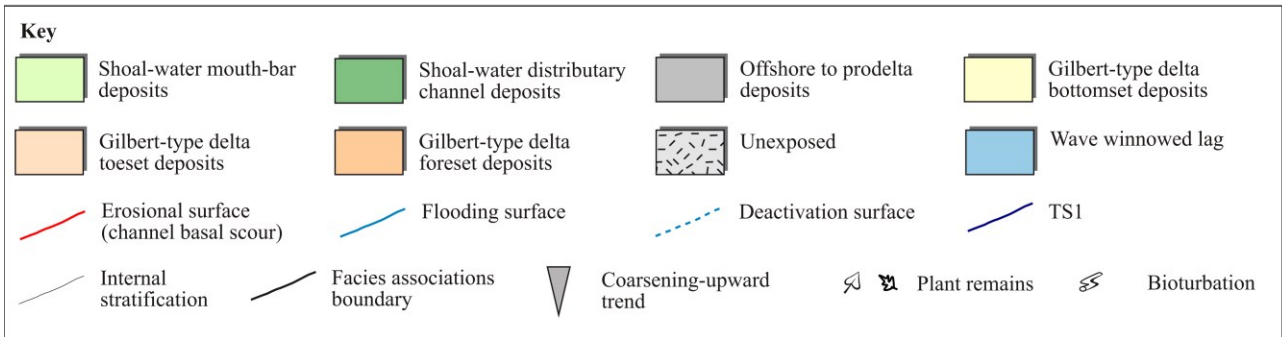
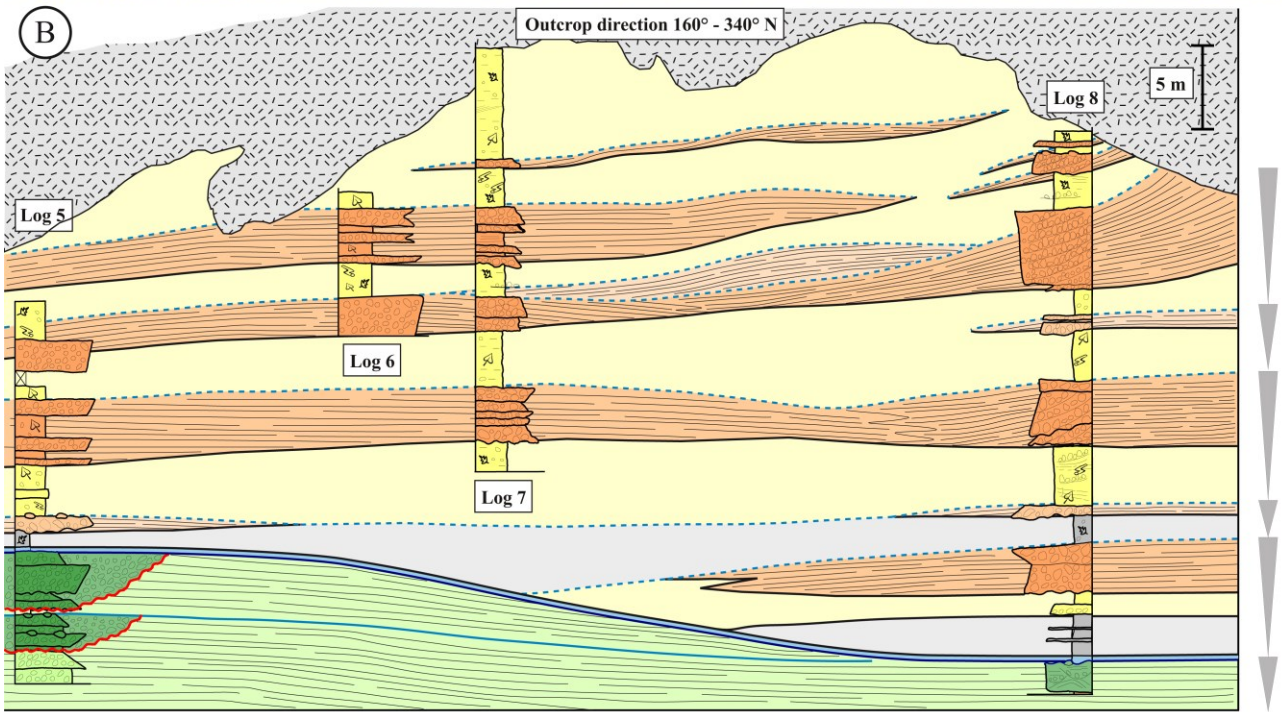
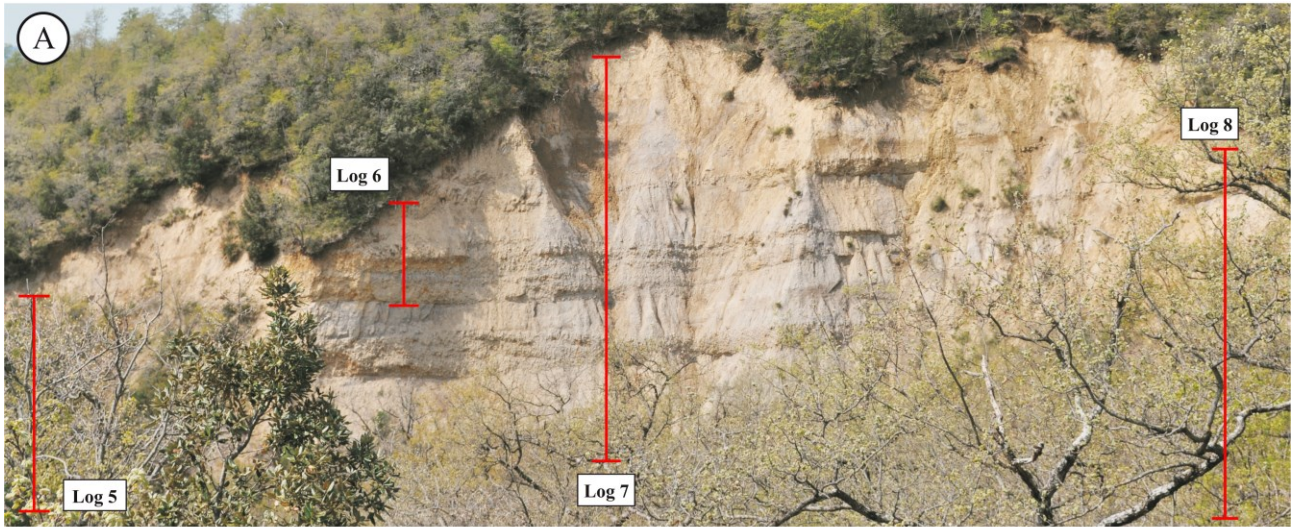


1045

1046

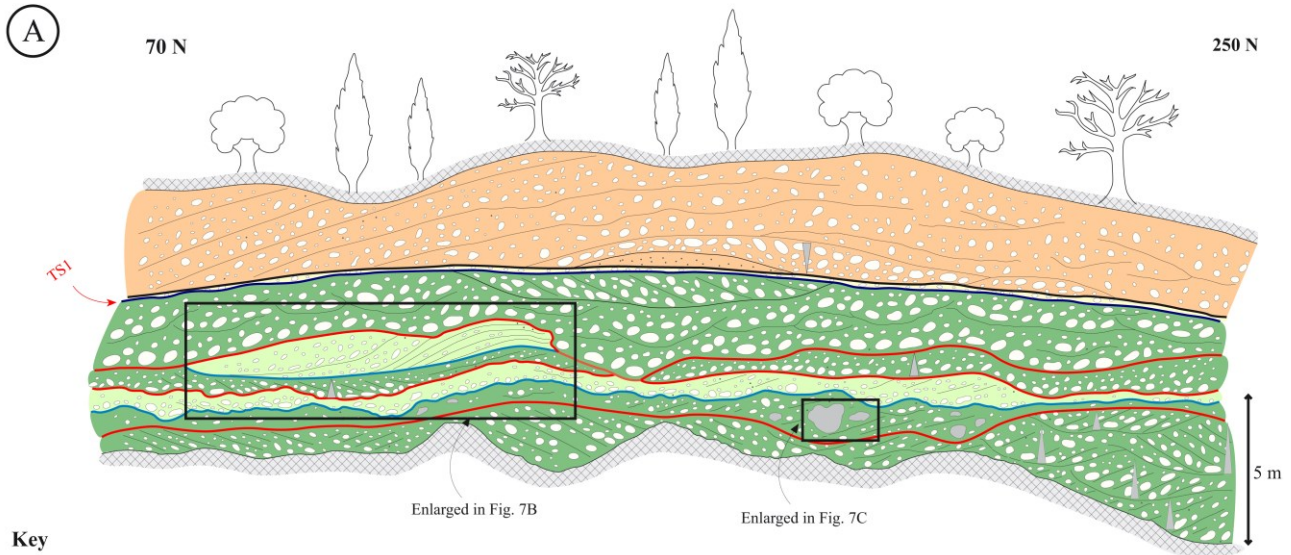






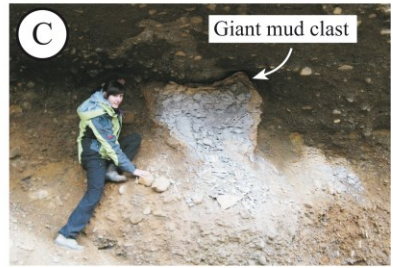
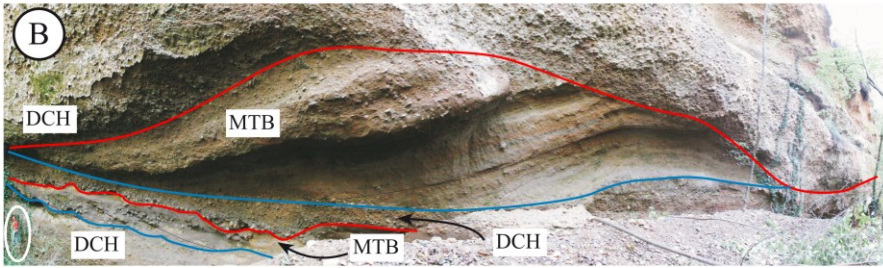
1050

1051



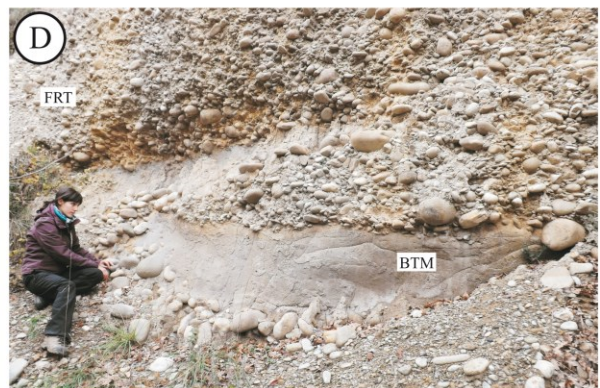
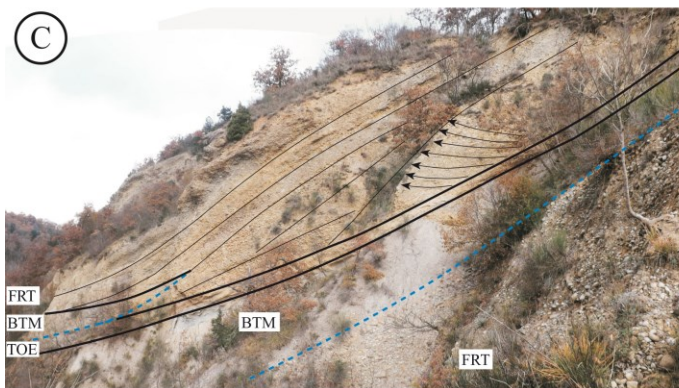
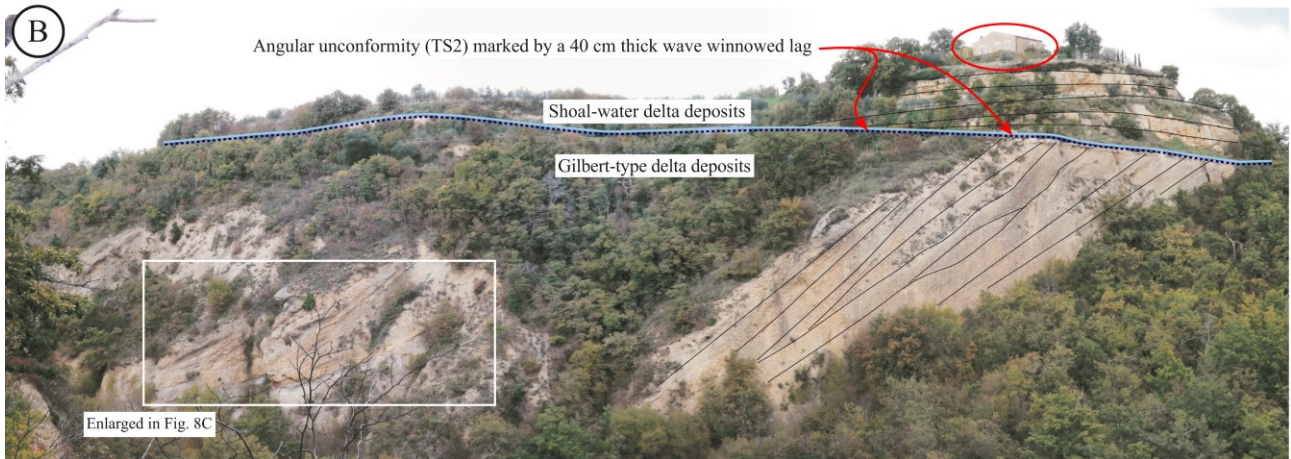
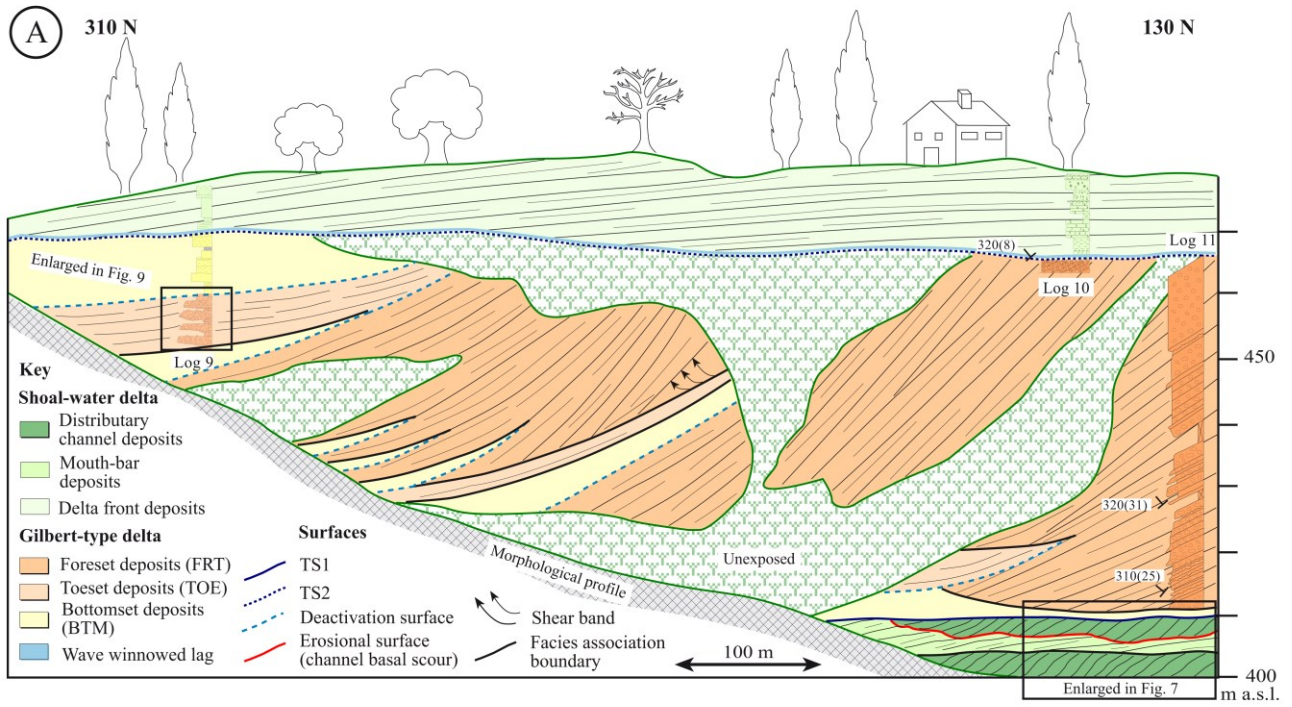
Key

- Distributary channel deposits (DCH)
- Mouth-bar deposits (MTB)
- Gilbert-type delta bottomset (BTM)
- Gilbert-type delta foreset (FRT)
- Flooding surface
- Erosional surface (channel basal scour)
- Facies associations boundary
- Internal stratification
- TS1
- Coarsening-upward trend
- Fining-upward trend



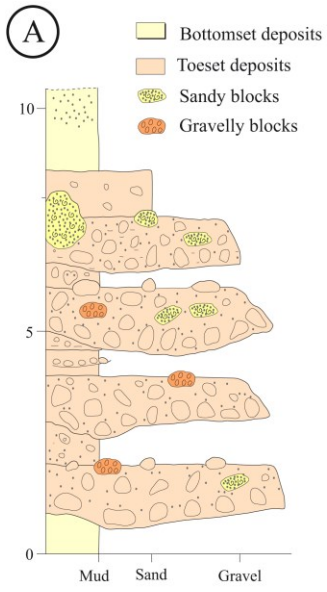
1052

1053



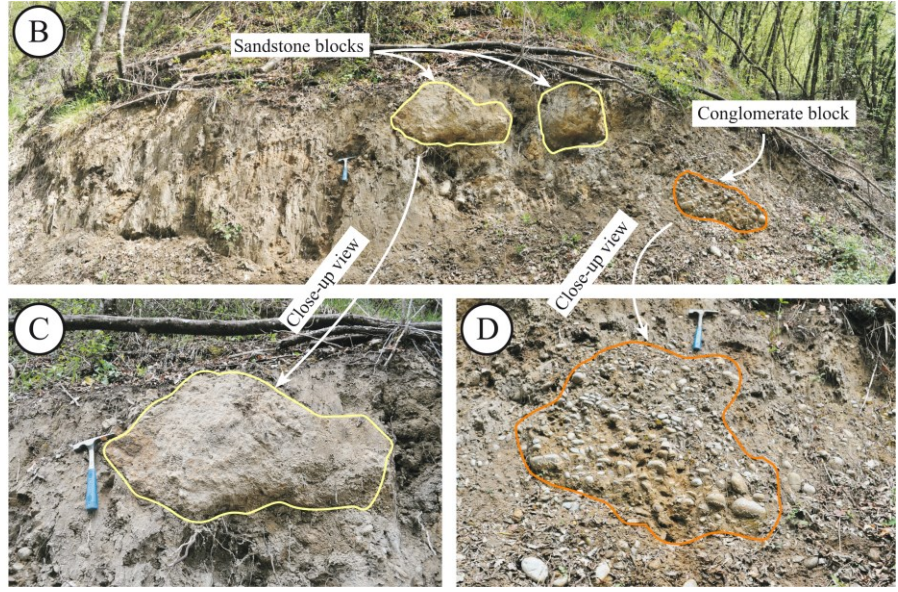
1054

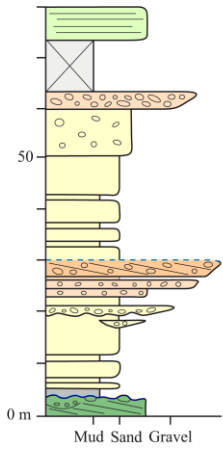
1055



1056

1057





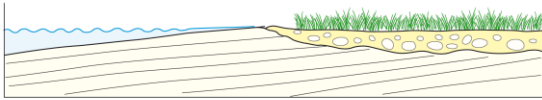
- Key**
- Shoal-water distributary channel deposits
 - Shoal-water mouth-bar deposits
 - Offshore to prodelta deposits
 - Gilbert-type delta bottomset deposits
 - Gilbert-type delta toeset deposits
 - Gilbert-type delta foreset deposits
 - Deactivation surface
 - TS1 + Wave winnowed lag

1058

1059

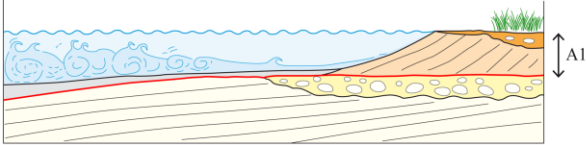
Stage 1

- Shoal-water delta progradation



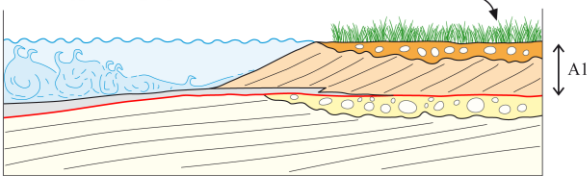
Stage 2

- Drowning of the shoal-water delta
- Gilbert-type delta inception



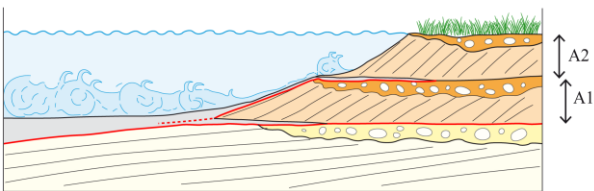
Stage 3

- Gilbert-type delta progradation



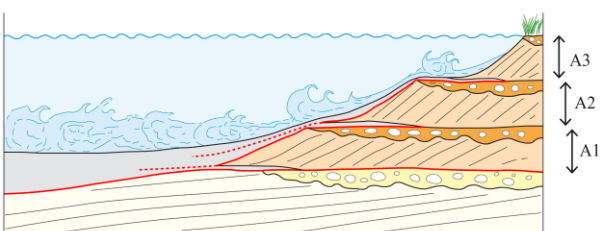
Stage 4

- Pulsating creation of accommodation space not counterbalanced by sediment supply
- Delta growth above the delta plain: aggradation and retrogradation



Stage 5

- Ongoing of Gilbert-type delta aggradation and retrogradation



Key

Shoal-water delta

- Mouth-bar deposits
- Distributary channel deposits

Gilbert-type delta

- Foreset deposits
- Topset deposits
- Bottomset to prodelta deposits

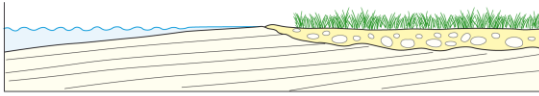
- Internal stratification
- Flooding surface
- Positive accommodation space variations

1060

1061

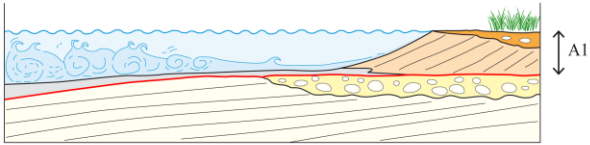
Stage 1

- Shoal-water delta progradation



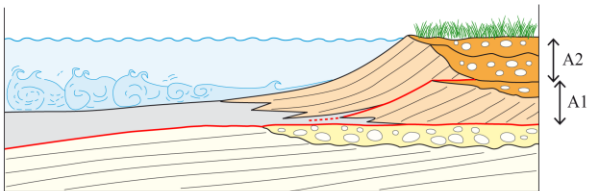
Stage 2

- Drowning of the shoal-water delta
- Gilbert-type delta growth and progradation



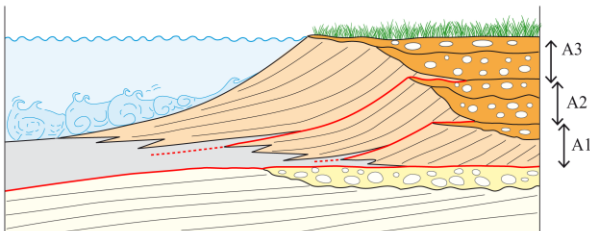
Stage 3

- Pulsating creation of accommodation space counterbalanced by sediment supply
- Gilbert-type delta aggradation and progradation



Stage 4

- Pulsating creation of accommodation space counterbalanced and overcome
by sediment supply
- Gilbert-type delta progradation and aggradation



Key

Shoal-water delta

- Mouth-bar deposits
- Distributary channel deposits

Gilbert-type delta

- Foreset deposits
- Topset deposits
- Bottomset to prodelta deposits
- Internal stratification
- Flooding surface
- Positive accommodation space variations